

1 Attenuation of pattern recognition receptor signaling is mediated by a MAP 2 kinase kinase kinase

3

4 Sharon C. Mithoe¹, Christina Ludwig², Michiel J.C. Pel¹, Mara Cucinotta¹, Alberto Casartelli¹, Malick
5 Mbengue³, Jan Sklenar³, Paul Derbyshire³, Silke Robatzek³, Corné M.J. Pieterse¹, Ruedi
6 Aebersold^{2,4} and Frank L.H. Menke^{1,3}

7 ¹ Department of Biology, Faculty of Science, Utrecht University, Padualaan 8 3584CH Utrecht, The Netherlands; ²
8 Department of Biology, Institute of Molecular Systems Biology, ETH Zürich, Wolfgang-Pauli-Str. 16, 8093 Zürich,
9 Switzerland; ³The Sainsbury Laboratory, Norwich Research Park, NR4 7UH Norwich, United Kingdom; ⁴Faculty of Science,
10 University of Zurich, 8093 Zurich, Switzerland.

11

12 Running title: MKKK7 negatively regulates FLS2 signaling

13

14 Abstract

15 Pattern recognition receptors (PRRs) play a key role in plant and animal innate immunity.
16 PRR binding of their cognate ligand triggers a signaling network and activates an
17 immune response. Activation of PRR signaling must be controlled prior to ligand binding
18 to prevent spurious signaling and immune activation. Flagellin perception in *Arabidopsis*
19 through FLAGELLIN-SENSITIVE 2 (FLS2) induces activation of mitogen activated
20 protein kinases (MAPKs) and immunity. However, the precise molecular mechanism that
21 connects activated FLS2 to downstream MAPK cascades remains unknown. Here we
22 report the identification of a differentially phosphorylated MAP kinase kinase kinase that
23 also interacts with FLS2. Using targeted proteomics and functional analysis we show that
24 MKKK7 negatively regulates flagellin-triggered signaling and basal immunity and this
25 requires phosphorylation of MKKK7 on specific serine residues. MKKK7 attenuates
26 MPK6 activity and defense gene expression. Moreover, MKKK7 suppresses the reactive
27 oxygen species burst downstream of FLS2, suggesting that MKKK7-mediated
28 attenuation of FLS2 signaling occurs through direct modulation of the FLS2 complex.

29

30 Synopsis

31 This study reports a MAP kinase kinase kinase as a negative regulator of pattern recognition
32 receptor signaling and immunity. MKKK7 represses FLS2 signaling upstream of MAPK activation
33 and reactive oxygen species burst.

- 34 · MKKK7 co-immunoprecipitates with FLS2
- 35 · MKKK7 is transiently phosphorylated in response to flagellin perception
- 36 · Phosphorylation of specific MKKK7 residues is required for its immunoregulatory function

37

This is the author manuscript accepted for publication and has undergone full peer review but has not been through the copyediting, typesetting, pagination and proofreading process, which may lead to differences between this version and the [Version of Record](#). Please cite this article as [doi: 10.15252/embr.201540806](https://doi.org/10.15252/embr.201540806)

1 Keywords: *Arabidopsis* / innate immunity / phosphorylation / signaling /targeted proteomics

2 **Introduction**

3 Initiation of basal plant defenses relies on the detection of pathogen-or microbe-associated
4 molecular patterns (PAMPs or MAMPs) through pattern recognition receptors (PRRs) [1].
5 One of the best-characterized plant PRRs is FLAGELLIN-SENSITIVE 2 (FLS2), a leucine-
6 rich repeat (LRR) receptor kinase, which together with co-receptor BRASSINOSTEROID
7 INSENSITIVE 1-ASSOCIATED KINASE 1 (BAK1) recognizes a conserved 22-amino acid
8 peptide (flg22) from bacterial flagellin [2-4]. PAMP perception induces immediate early
9 responses, including the production of reactive oxygen species (ROS), ion fluxes across the
10 plasma membrane, mitogen-activated protein kinase (MAPK) activation as well as later
11 responses, such as activation of defense-related genes [5-8]. These immune responses
12 eventually lead to a first line of defense called PAMP-triggered immunity (PTI). Successful
13 pathogens overcome PTI by secreting or injecting a set of effectors into the host, which
14 suppress key steps of PTI, resulting in interference of plant defense [9]. In turn, plants have
15 evolved resistance (R) proteins that monitor the host targets of these effector molecules.
16 Perception of effector-mediated modulation of these host target proteins leads to a strong
17 defense response known as effector-triggered immunity (ETI) [9-13].
18 Tremendous progress has been made in unraveling molecular mechanisms of the signaling
19 events leading to PTI and ETI, suggesting that they rely on similar components [6, 13].
20 Protein phosphorylation is essential in PRR signaling and for the activation of several
21 PAMP-activated MAPK cascades [5, 14-16]. However, what connects upstream PRRs to
22 downstream MAP kinase activation has remained an open question. Moreover, the nature of
23 the MAP kinase kinase kinase (MAPKKK) acting to mediate flg22-induced MAPK activation
24 remains a matter of debate [17, 18]. Only recently has the first gap been bridged between
25 PRR activation and ROS burst, an early defense response mediated by NADPH oxidase
26 RBOHD [19, 20]. In addition to positive regulation, mediated in part by phosphorylation, PRR
27 complexes and their downstream signaling components must be under negative regulation
28 to prevent activation in the absence of PAMPs and to allow rapid deactivation after PAMP
29 signaling has been initiated [6]. Recent examples of negative regulators of *Arabidopsis* PTI
30 include protein phosphatase PP2A, involved in down-regulating PAMP triggered signaling
31 [21] and the BAK1-INTERACTING RECEPTOR-LIKE KINASE 2 (BIR2) that prevents
32 formation of active signaling complexes prior to PAMP binding [22].
33 We, and others, have previously undertaken several large-scale phosphoproteomics
34 approaches to identify proteins involved in early defense-related signaling events [16, 23-
35 25]. In our previous quantitative phosphoproteomic study, swift changes in phosphorylation
36 of membrane-associated proteins were analyzed in response to flg22 and the fungal PAMP
37 xylanase [23]. We identified a large set of differentially phosphorylated proteins, some of

1 which were subsequently characterized as important signaling components, including
2 receptor-like cytoplasmic kinase BOTRYTIS-INDUCED KINASE1 (BIK1), RBOHD [19, 20,
3 24, 26, 27] and RPM1-INTERACTING PROTEIN 4 (RIN4) [28]. We also identified several
4 members of the MAPKKK family as differentially phosphorylated and describe the functional
5 analysis of one of these MAPKKKs here.

6 Comprising 80 members, the MAPKKK family is the largest group of MAPK pathway
7 components, however relatively little is known about their function in plants [29]. To date, in-
8 depth functional analysis has been performed for only a few MAPKKK family members [30,
9 31]. Sequence analysis of the protein kinase catalytic domain revealed that *Arabidopsis*
10 MAPKKKs fall into two major subtypes: MEKKs and RAF-like kinases [32]. MEKK subfamily
11 members studied in more detail include *Arabidopsis* MEKK1, which activates MKK4 and
12 MKK5 [18] as well as MKK1 and MKK2 [17, 33] in response to flg22 sensing. The orthologue
13 of MEKK1 in *Nicotiana tabacum* (tobacco) NPK1, is involved in innate immunity and
14 cytokinesis [30, 34] and tobacco MAPKKK α and tomato MAPKKK ϵ are involved in regulating
15 pathogen-induced cell death [35-37].

16 Our previous work has identified *Arabidopsis* MKKK7 (At3g13530, also known as
17 MAP3Ke1), as a membrane-associated phosphoprotein [23]. Here we report the interaction
18 of MKKK7 with FLS2 and outline its role in the attenuation of FLS2-mediated signaling. We
19 show, using selective reaction monitoring (SRM), that several Serine residues in MKKK7 are
20 differentially phosphorylated in response to flg22 sensing, and provide evidence that
21 phosphorylation of two Serine residues is important for the regulation of MKKK7 function.
22 Our work suggests that MKKK7 is a negative regulator of PAMP signaling and basal
23 immunity in *Arabidopsis*, and acts early in PAMP signaling through its association with the
24 FLS2 complex.

26 Results

28 FLS2 interacts with MKKK7

29 To identify immediate early signaling components in the FLS2 pathway we performed co-
30 immunoprecipitation (co-IP) experiments with FLS2-GFP as bait in *Arabidopsis*. We
31 immunoprecipitated FLS2-GFP with anti-GFP antibody coated beads and analyzed co-
32 precipitated proteins by liquid chromatography tandem mass spectrometry (LC-MS/MS).
33 Among the proteins pulled down in the FLS2-GFP IP, we identified MKKK7 (At3g13530)
34 through five peptides (Table I, Figure EV1 and Dataset EV1). The interaction appeared
35 specific, as only one MKKK7 peptide with a low Mascot score was identified in one of three
36 replicas of a similar co-IP using plasma membrane (PM) localized Lti6B-GFP [38] as a
37 control (Table I and Dataset EV1). MKKK7 is a plasma membrane-associated protein that

1 was previously identified in our screen for differentially phosphorylated proteins after flg22
2 treatment [23]. MKKK7 is a MAPKKK with a typical S/T kinase domain and is classified as a
3 subgroup A4 of the MEKK subfamily [32]. Since we identified MKKK7 in two independent
4 screens for signaling proteins in the FLS2 pathway we investigated its role in FLS2-
5 dependent signaling in more detail. We first verified the FLS2-MKKK7 association by
6 repeating the co-IP with a GFP-binding protein in *Arabidopsis* transgenic plants expressing a
7 functional YFP-MKKK7 fusion protein [39]. Both prior to stimulation with flg22 and at early
8 time points post flg22 treatment, FLS2 co-immunoprecipitated with YFP-MKKK7 but not with
9 Lti6B-GFP (Figure 1). These reciprocal co-IP results confirm the formation of a specific
10 stable interaction between MKKK7 and FLS2.

11

12 **Flg22-triggered changes in MKKK7 phosphorylation**

13 We previously identified MKKK7 as a phospho-protein using a shotgun proteomics approach
14 (Figure EV2, [23]). We were able to reproducibly quantify phosphorylation for two Serine
15 residues (S⁵⁰³, S⁷⁷⁵), but none of these residues were differentially phosphorylated in
16 response to PAMP perception [23]. We also measured changes of phosphorylation on two
17 additional residues (S⁴⁵² and S⁸⁵⁴), but for these residues the shotgun proteomics approach
18 prevented us from confidently determining whether these changes were PAMP-induced.
19 These phosphorylated Serine residues (pS⁴⁵², pS⁵⁰³, pS⁷⁷⁵ and pS⁸⁵⁴) and an additional
20 phosphorylated Serine residue (pS³³⁷) [40], are located in the central domain of the protein,
21 outside the kinase domain, in a region containing an armadillo (ARM)/HEAT repeat domain
22 found in MKKK7 (Figure EV2) and homologous MAPKKKs in other plant species. The first
23 three phosphorylated Serine residues (S³³⁷, S⁴⁵² and S⁵⁰³) are conserved in MKKK7
24 homologues from *Brassicaceae* species, but not in more distantly related species such as
25 tomato and apple (Figure EV3). The other two phosphorylated residues (S⁷⁷⁵ and S⁸⁵²) are
26 conserved in closely related species as well as more distantly related species.

27 To reproducibly quantify phosphorylation of these 5 Serine residues in MKKK7 and several
28 other residues in additional MAPK cascade members in response to flg22 perception, we
29 developed selected reaction monitoring (SRM) assays using synthetic phosphopeptides as
30 reference molecules (Dataset EV2). SRM assays were set up using light (¹⁴N) synthetic
31 phosphopeptides and detection of the corresponding heavy (¹⁵N) endogenous
32 phosphopeptides was validated in phospho-enriched samples from metabolically labeled
33 *Arabidopsis* cell cultures. Relative quantification was done by spiking the ¹⁵N samples with
34 the light synthetic phosphopeptides and expressing changes in phosphorylation as a ratio of
35 heavy endogenous phosphopeptide over light synthetic phosphopeptide.

36 In phospho-enriched total extracts of cultured *Arabidopsis* cells, analyzed at 0, 5, 10, 20 and
37 30 minutes after flg22 treatment, we reliably quantified three out of five MKKK7

1 phosphopeptides, containing pS residues at position S⁴⁵², S⁷⁷⁵ and S³³⁷ (Figure 2A to C)
2 while phosphorylation of S⁵⁰³ and S⁸⁵² could only be detected in the light synthetic peptides
3 but not as heavy endogenous phosphopeptides. Temporal analysis in response to flg22
4 treatment revealed a sharp transient differential phosphorylation for S⁴⁵² at 5 min post-
5 induction (Figure 2A). Differential phosphorylation of S⁷⁷⁵ was more gradual, suggesting the
6 involvement of different upstream kinases (Figure 2B). The third quantified S³³⁷ showed no
7 significant increase in phosphorylation in response to flg22 treatment (Figure 2C). As
8 expected, temporal analysis of defense-associated MAP kinase MPK6, showed a swift
9 increase in phosphorylation of both T²²⁰ and Y²²² residues in the activation loop, consistent
10 with its rapid and transient activation in response to flg22 (Figure 2E, Dataset EV2 and
11 Figure EV4A) [16, 23, 41]. It is interesting to note here that we also observed a stable
12 increase in phosphorylation for only the Y²²² residue of MPK6 (Figure 2D and Figure EV4A).
13 We measured similar changes in phosphorylation for MPK3 as well (Figure EV4B). Recent
14 work on animal ERK2 shows that MAPKs get sequentially phosphorylated by the upstream
15 MAPK kinase, first on Tyrosine and then followed by phosphorylation on Threonine [42].
16 Only doubly phosphorylated ERK2 is activated while monophosphorylated ERK2 is inactive
17 [42]. Our data on MPK3 and MPK6 phosphorylation are consistent with this as we find very
18 little evidence for monophosphorylation on Threonine only (Figure EV4) and suggests that
19 MPK3 and MPK6 are also sequentially phosphorylated on Tyrosine, followed by
20 phosphorylation on Threonine. Another phosphopeptide, corresponding to MAP4K5 also
21 showed a rapid increase and sustained differential phosphorylation on S⁶⁵³ residue (Figure
22 2F). To ensure that the observed changes in phosphorylation are due to flg22 treatment, the
23 relative abundance of several other phosphopeptides corresponding to additional MAPK
24 members was also monitored. As shown in Figure 2 (G-I), selected phosphopeptides
25 corresponding to MPK17, MAP4K5 and MKK1 showed no statistically significant changes in
26 phosphorylation. Overall the data shows that our SRM assays can detect flg22-induced
27 changes in the relative abundance of selected phosphopeptides with great sensitivity and
28 reproducibility. This allowed the quantification of relatively small changes in phosphorylation
29 in MKKK7 phosphopeptides, while at the same time demonstrating that other
30 phosphopeptides remain constant over the course of the flg22 treatment. Furthermore, our
31 data suggests a specific and complex phosphorylation pattern of MKKK7 in response to
32 flg22 perception, consistent with a role in signal transduction.

33

34 **MKKK7 attenuates flg22-induced MAPK activation**

35 The interaction between MKKK7 and FLS2 and the flg22-triggered differential
36 phosphorylation suggest that MKKK7 may be involved in the modulation of flg22 signaling at
37 the level of FLS2 or immediately downstream of FLS2. To test the activation of downstream

1 MAPKs in a *mkkk7* loss-of function mutant, we identified a T-DNA insertion mutant allele of
2 *MKKK7* (Salk_133360) (Appendix Figure S1A and B) and confirmed the insertion by PCR
3 with gene-specific primers (Appendix Figure S1C upper panel). *MKKK7* transcript level in
4 *mkkk7* was shown by quantitative RT-PCR (qRT-PCR) to be reduced to background levels
5 (Appendix Figure S1C, lower panel), confirming *mkkk7* as a knock-out mutant.

6 When *mkkk7* seedlings were incubated for up to 30 min with 1 μ M flg22, we observed
7 induction of MAPK phosphorylation for MPK3, MPK4/11 and MPK6 with similar kinetics as in
8 Col-0 (Figure 3A upper panel). As shown, MPK4/11 and MPK3 were transiently
9 phosphorylated in Col-0 and *mkkk7* after treatment with flg22 (Figure 3A, upper panel).

10 There were minor differences observed in MPK4/11 and MPK3 phosphorylation in *mkkk7* in
11 the observed time frame, with slightly higher phosphorylation in *mkkk7* at 10 min after
12 induction with flg22. Interestingly, MPK6 showed enhanced phosphorylation in *mkkk7* at
13 both 10 and 30 min after induction with flg22. We observed this enhanced MPK6
14 phosphorylation in three independent biological replicates. We verified equal loading of the
15 proteins using an α -Actin antibody (Figure 3A, lower panel). To confirm that the differences
16 in MPK6 phosphoprotein levels were related to changes in the phosphorylation status of
17 MPK6 and not to an increase in MPK6 protein amount, a duplicate immuno-blot was run with
18 identical samples from flg22-treated Col-0 and *mkkk7* seedlings. The specific α -MPK6
19 antibody showed that the MPK6 protein levels were unaltered after flg22 induction (Appendix
20 Figure S2B upper panel), while probing the blot with α -Actin antibody confirmed equal
21 loading (Appendix Figure S2B lower panel). Together, these data show that the enhanced
22 phosphorylation of MPK6 detected in flg22-treated *mkkk7* seedlings is due to differences in
23 phosphorylation, while MPK6 protein levels remain constant.

24 The results of the immunoblot were encouraging, but due to the small differences not
25 conclusive. We therefore used the SRM assays we had set up to verify the enhanced
26 phosphorylation status of MPK6 in *mkkk7* seedlings. We used the same SRM assays to
27 detect phosphopeptides as before but directly compared light (14 N) endogenous
28 phosphopeptides from *mkkk7* seedling samples to the heavy (15 N) phosphopeptides from
29 the metabolically labeled Col-0 seedlings. Consistent with the Western blot results, the
30 doubly phosphorylated peptide (VTSEDFMT[+80.0]EY[+80.0]VVTR) corresponding to the
31 activation loop of MPK6 was detected at about 1.5 fold higher level in *mkkk7* as compared to
32 Col-0 at 10 min post-induction with 1 μ M flg22 (Figure 3B). Other versions of MPK6
33 phosphopeptides (pT²²⁰ or pY²²²) as well as phosphopeptides for MPK3 (pT¹⁹⁶, pY¹⁹⁸ and
34 pT¹⁹⁶/pY¹⁹⁸) could not be measured in phospho-enriched samples from Col-0 or *mkkk7*
35 seedlings, despite the fact that we could detect several of these phosphopeptides in cell
36 culture samples (Figure EV4). Several other phosphopeptides, including those from other
37 MAPK cascade proteins involved in defense signaling, such as MPK4 and MAP4K5, did not

1 show significant differences in flg22-induced phosphorylation between Col-0 and *mkkk7*
2 (Figure 3B and Dataset EV2). Additionally, three phosphopeptides corresponding to MKKK7
3 could be measured in Col-0. However these were not detectable above background in
4 *mkkk7*, suggesting a significant reduction in MKKK7 (phospho)-protein consistent with
5 reduced *MKKK7* mRNA levels in this T-DNA insertion mutant (Figure 3B). Our results show
6 that in *mkkk7*, the flg22-induced level of phosphorylation and activation of MPK6 is
7 specifically enhanced, indicating that MKKK7 attenuates MPK6 activation in FLS2-
8 dependent signaling.

10 **MKKK7 represses defense gene expression**

11 To verify whether changes in MPK6 phosphorylation in *mkkk7* also lead to changes in
12 defense gene expression, we compared flg22-induced early defense gene expression in
13 *mkkk7* to Col-0. We used transient expression of promoter:Luciferase (LUC) constructs in
14 mesophyll protoplasts to test flg22-induced *WRKY29* and *FRK1* expression [18]. Treatment
15 of Col-0 and *mkkk7* protoplasts with flg22 activated *WRKY29* and *FRK1* expression, but to a
16 substantially higher level in *mkkk7* compared to Col-0 (Figure 4A), in particular for *FRK1*.
17 The observations in mesophyll protoplasts were confirmed by qRT-PCR analysis of
18 *WRKY29* and *FRK1* mRNA levels in leaf strips of Col-0 and *mkkk7* plants (Figure 4B and C).
19 We observed enhanced basal and flg22-induced *WRKY29* and *FRK1* gene expression in
20 *mkkk7* relative to Col-0 (Figure 4B and C), indicating sustained defense gene activation in
21 *mkkk7* leaf strips. This suggests that loss of MKKK7 protein enhances early defense gene
22 expression, consistent with enhanced MPK6 activation.

24 **Phosphorylation of MKKK7 is required to attenuate flg22-induced defense gene 25 expression**

26 We demonstrated enhanced MAPK activity and defense gene expression in the *mkkk7*
27 mutant background. To complement these results we used a gain-of-function approach and
28 we transiently overexpressed *MKKK7* by co-transfection in protoplasts to test flg22-induced
29 defense gene expression. Co-transfecting *p35S:MKKK7* attenuates flg22-induced *WRKY29*
30 expression as compared to the flg22-induced *WRKY29* expression in protoplasts
31 transformed with our negative control (*p35S:GFP*) (Figure 5A). We obtained similar results
32 when we analyzed *FRK1* expression in this system (Figure EV5). These results are
33 consistent with our loss-of-function *mkkk7* data and suggest that higher levels of MKKK7 can
34 suppress flg22-triggered defense gene activation.

35 Since MKKK7 is a phospho-protein and shows changes in phosphorylation in response to
36 flg22, we tested whether phosphorylation is required for its function as a negative regulator
37 of flg22-induced gene expression. We initially identified two Serine residues (S⁴⁵² and S⁸⁵⁴)

1 as potential PAMP-induced phospho-sites in our shotgun data set. We were able to verify
2 differential phosphorylation by SRM for S⁴⁵² but not for S⁸⁵⁴. While we also targeted S⁸⁵⁴ for
3 phospho-SRM analysis, and were able to measure the synthetic phosphopeptide, we were
4 unable to confidently detect the endogenous version of the corresponding phosphopeptide
5 above background. Since the shotgun data implicated both S⁴⁵² and S⁸⁵⁴ and the similarity of
6 the residues surrounding S⁴⁵² (pSSVS) and S⁸⁵⁴ (pSSVA) suggests that they may be
7 targeted by the same kinase, we decided to mutate both residues. Using site-directed
8 mutagenesis we changed both Serine residues into Alanine (A) or Aspartate (D), to create
9 non-phosphorylatable (*MKKK7^{AA}*) and phosphomimetic (*MKKK7^{DD}*) versions (Figure 5B).
10 Co-transfection of *p35S:MKKK7^{AA}* did not attenuate flg22-induced *WRKY29* gene
11 expression (Figure 5A) or flg22-induced *FRK1* gene expression (Figure EV5), showing a
12 response equal to the negative control transformed protoplasts. When *p35S:MKKK7^{DD}* was
13 co-transfected, a nearly complete loss of flg22-responsive *WRKY29* (Figure 5A) and *FRK1*
14 (Figure EV5) gene expression was observed. Thus, co-transfection of *MKKK7* or *MKKK7^{DD}*,
15 but not *MKKK7^{AA}*, results in suppression the flg22-induced early defense gene expression.
16 These data show that phosphorylation of MKKK7 on one or both Serine residues may be
17 required for attenuation of flg22-induced defense gene expression.

18

19 **MKKK7 represses basal immune response**

20 To test whether MKKK7 regulates the basal immune responses in *Arabidopsis*, we first
21 evaluated *Pseudomonas syringae* pv. *tomato* DC3000 (*Pst*) induced disease symptom
22 development in *mkkk7* compared with Col-0 (Figure 6A). We dipped plants into a suspension
23 of virulent *Pst* and scored disease symptoms, including water soaked lesions and chlorosis
24 on leaves 3 days after inoculation (dpi). In three independent experiments the percentage of
25 leaves showing disease symptoms was significantly less in *mkkk7* compared to Col-0
26 (Figure 6A), suggesting that *mkkk7* is less susceptible to this virulent pathogen than Col-0.

27 To distinguish between delayed disease symptom development in *mkkk7* and actual
28 enhanced resistance to virulent *Pst* we quantified bacterial growth in the loss-of-function
29 mutant *mkkk7* in four independent experiments. At 3 dpi, the bacterial titer in leaves of
30 *mkkk7* was significantly lower compared to Col-0 (Figure 6B). We also quantified the
31 bacterial growth in a complemented transgenic line carrying *p35S:MKKK7-GFP* in the *mkkk7*
32 background in two of the independent experiments mentioned above. Expression of
33 *p35S:MKKK7-GFP* in the *mkkk7* background did not cause any noticeable phenotype prior
34 to infection (Appendix Figure S3A and S3B). No significant effect of constitutive
35 overexpression of *MKKK7* in *mkkk7* on growth of *Pst* could be observed (Figure 6B).
36 However, overexpressing *MKKK7* in the *mkkk7* background enhanced disease symptom
37 development at an earlier stage (Figure EV 6A). These results support of the idea that the

1 decrease in disease symptoms seen in infected *mkkk7* is caused by a more effective
2 restriction of bacterial growth compared to Col-0 and that MKKK7 acts a suppressor of basal
3 immunity.

5 **Phosphorylation of MKKK7 is necessary for suppression of basal immunity**

6 Overexpression of *MKKK7* and *MKKK7^{DD}* in protoplasts resulted in substantial attenuation of
7 flg22-triggered defense gene expression (Figure 5A and Figure EV5). To test the importance
8 of phosphorylation of MKKK7 in suppression of basal immunity, we made transgenic lines
9 expressing *MKKK7^{AA}* and *MKKK7^{DD}*. Since we noticed that constitutive overexpression of
10 *MKKK7* in Col-0 background resulted in a spectrum of phenotypes under normal growth
11 conditions (Appendix Figure S3A), we used an estradiol inducible promoter [43] to drive
12 expression of *MKKK7^{AA}* and *MKKK7^{DD}* (*ind-MKKK7^{AA}*, *ind-MKKK7^{DD}*).

13 Two independent *ind-MKKK7^{AA}* and *ind-MKKK7^{DD}* transgenic lines were dip-inoculated with
14 virulent *Pst*, 24 hours after spraying with an estradiol solution. In Col-0 plants the percentage
15 of leaves with disease symptoms was 51% at 3 dpi (Figure 6C). In *ind-MKKK7^{AA}* disease
16 symptom development was comparable to Col-0. Overexpression of the phospho-mimic
17 version of *MKKK7* (*ind-MKKK7^{DD}*) resulted in a significant increase in disease symptoms
18 (Figure 6C). To show that the *ind-MKKK7^{DD}* lines are indeed more susceptible to *Pst*
19 infection, we also infiltrated leaves with a low titer of *Pst*. At 2 days post inoculation the level
20 of bacteria was higher in both transgenic lines as compared to the Col-0 control (Figure
21 EV6B). These observations support the requirement of phosphorylation of MKKK7 on one or
22 both S residues (S⁴⁵² and S⁸⁵⁴) to suppress basal immunity.

24 **MKKK7 attenuates FLS2-mediated ROS burst**

25 MKKK7 mediated attenuation of MPK6 activation and defense gene expression may be
26 sufficient to cause the change in basal immune response. However, recently it was
27 demonstrated that ROS contributes to resistance to *Pst* infection [19, 20] and that ROS burst
28 and MAPK activation are two independent early signaling events [44]. ROS production by
29 RBOHD in response to flg22 was recently shown to require phosphorylation by BIK1 [19].
30 Both RBOHD and BIK1 interact with FLS2, which suggest that flg22 perception by FLS2 is
31 directly coupled to RBOHD mediated ROS burst through BIK1 action. Since MKKK7 also
32 interacts with FLS2, the observed changes in basal immunity could be partly due to altered
33 ROS production in lines with changed expression levels of MKKK7. Flg22-triggered ROS
34 burst in *mkkk7*, shows no significant increase as compared to Col-0 (Figure 7A). In support
35 of our model, overexpression of *MKKK7^{AA}* enhanced ROS burst in one of the lines (Figure
36 7B), possibly indicating a dominant negative effect, while overexpression of *MKKK7^{DD}*
37 suppressed ROS production (Figure 7C).

1 Taken together our results demonstrate that MKKK7-mediated attenuation of FLS2 signaling
2 modulates ROS production, MPK6 activation and downstream defense gene expression and
3 ultimately basal immunity. Since both ROS burst and MAPK activation are affected by
4 changes in MKKK7 protein level and phosphorylation, our results are consistent with a
5 hypothesis in which MKKK7 affects attenuation of FLS2 complex output.

6 7 **Discussion**

8
9 Understanding the regulation of PRR signaling and downstream PTI has seen tremendous
10 progress over the last few years [6]. While many of the components recently identified play a
11 positive role in PRR signaling, several negative regulators have also been uncovered. Here
12 we describe a novel negative regulator of FLS2-mediated signaling and show its role in
13 attenuation of early defense responses and immunity. MKKK7 was identified in two
14 proteomics based screens for FLS2 signaling components, one for FLS2 interacting proteins
15 (described here) and the other for flg22-induced phosphorylation of PM associated proteins
16 [23]. Significant numbers of differentially phosphorylated proteins were identified in response
17 to PAMP perception [23, 24, 41] including proteins important for PTI signaling such as BIK1
18 and RBOHD [23]. However, relatively few of these phosphorylation sites have been
19 described as functionally relevant. The most notable exception is RBOHD, which is
20 phosphorylated on specific residues by BIK1, including one Serine residue that is required
21 for its subsequent activation by other kinases [19]. While functional analysis is labor
22 intensive, it is also hampered by the inability to reproducibly measure and quantify the same
23 phosphorylated peptide in replicate experiments by shotgun proteomics approaches and the
24 general lack of phosphopeptide specific antibodies. To address this problem we have
25 developed a quantitative MS-based approach in which we combined SRM with ¹⁵N
26 metabolic labeling to determine changes in phosphorylation on specific residues of MKKK7
27 after flg22 treatment. This approach relies on *a priori* knowledge of the targeted
28 phosphopeptide, during LC separation and fragmentation in the mass spectrometer, and
29 requires generation of a mass spectrometric assay for each targeted (phospho-) peptide. We
30 have made use of synthetic phospho-peptides to set up the SRM assays for each peptide,
31 allowing us to positively identify the correct set of transitions (pairs of precursor and
32 fragment ions) and accurately determine the retention time of each peptide. Both these
33 parameters are essential to accurately select and quantify the correct peaks. These assays
34 can then be applied reproducibly to quantify the abundance of the targeted phospho-peptide.
35 This allowed us to confidently identify residues with a potential role in the regulation of
36 MKKK7 function, in addition to quantify changes in other phosphoproteins in response to
37 flg22 at the same time. We verified the importance of phosphorylation of MKKK7 on S⁴⁵² and

1 S⁸⁵⁴ by changing to either non-phosphorylatable Alanine or phospho-mimetic Aspartate
2 residues, followed by measuring changes in several different defense-related outputs. SRM
3 in combination with metabolic labeling also allowed us to accurately quantify changes in
4 phosphorylation of key MAP kinase cascade proteins in ¹⁴N labeled *mkkk7* seedlings
5 compared to ¹⁵N labeled Col-0 seedlings. This enabled us to unequivocally show important
6 changes in phosphorylation of this key defense signaling proteins in *mkkk7*, while the level
7 of flg22-induced phosphorylation of most other monitored proteins did not change as
8 compared to the Col-0 control.

9 There are more than 60 MAPKKK members in *Arabidopsis* [32] but to date, only one plant
10 MAPKKK involved in defense responses has been described as a protein regulated by
11 phosphorylation. SIMAPKKK α abundance and activity are stabilized by phosphorylation on a
12 C-terminal serine residue and binding of the pS residue by a 14-3-3 protein [45]. We show
13 here that *Arabidopsis* MKKK7 is differentially phosphorylated in response to flg22 and that
14 one or two of the identified pS residues (pS⁴⁵² and pS⁸⁵⁴) are important for its function as a
15 negative regulator of FLS2 signaling. The combined biochemical results and phospho-SRM
16 data are supported by our transient expression experiments in mesophyll protoplasts. The
17 transient expression system in mesophyll protoplasts is an excellent model system in which
18 flg22 perception leads to the activation of *Arabidopsis* MPK3 and MPK6 upstream of
19 *WRKY29* and *FRK1* expression [18]. Flg22-induced MPK3 and MPK6 activation is essential
20 for normal induction of expression of these genes, as overexpression of phosphothreonine
21 lyase effector proteins HopAI1 or SpVC in mesophyll protoplasts completely blocks flg22-
22 induced MAPK activation and downstream defense gene expression (Mithoe and Menke,
23 unpublished data) [46]. The marker genes *WRKY29* and *FRK1* can thus be used as a proxy
24 for MAP kinase activation in *Arabidopsis*. We observed that flg22-induced defense gene
25 expression was effectively repressed when *MKKK7* or *MKKK7^{DD}* were co-transfected into
26 protoplasts (Figure 5A and Figure EV5). Co-transfection of *MKKK7^{AA}* did not block
27 responsiveness to flg22. These results point towards a direct connection between the
28 phosphorylation status of MKKK7 and its role as a suppressor of FLS2-dependent MAPK
29 activation.

30 The role of MKKK7 as a negative regulator of FLS2 signaling and flg22-triggered MPK6
31 activation is also supported by available evidence for the positive role of MPK6 in basal
32 immunity or PTI [18, 47-49]. *MPK6*-silenced lines displayed an enhanced susceptibility
33 against avirulent and virulent strains of *P. syringae* [49] and a MEKK1-MKK4/MKK5-
34 MPK3/MPK6 cascade was shown to be required for PTI against virulent bacterial and fungal
35 pathogens [18]. Also, *Arabidopsis* MAP kinase phosphatase1 (MKP1), which targets and
36 dephosphorylates MPK6, is observed as a negative regulator of PAMP responses and
37 bacterial resistance [47, 48]. Similarly, *mkkk7* displayed an increase in resistance against

1 virulent *Pst*, while overexpression of *MKKK7^{DD}*, but not *MKKK7^{AA}*, resulted in enhanced
2 susceptibility to virulent *Pst*. When all data is taken into consideration, it is likely that MKKK7
3 directly attenuates the MPK3/MPK6 cascade through interaction with FLS2, affecting flg22-
4 induced defense signaling and PTI. As such, reduction of active MKKK7 protein in *mkkk7*
5 could lead to a state of priming, in which the cells respond faster to PAMP perception.
6 Priming of stress response has been shown to require MPK3 and MPK6 in *Arabidopsis* [50]
7 and *mkkk7* with slightly altered levels of MPK6 activity may actually indicate a primed state.
8 Similar priming phenotypes were recently also reported for *pp2a* subunit mutants, which did
9 not display constitutive defense responses, but responded stronger to PAMPs [21].

10 The recent identification of several negative regulators of PTI signaling is compelling
11 evidence for the strict regulation of signaling cascades prior to PAMP perception and
12 immediately after the signal has been transduced. This ensures a timely and dosed
13 response and allows coordinated control of growth and defense responses. Negative
14 regulation of PTI signaling occurs at different levels with some proteins affecting complex
15 formation, such as the pseudokinase BIR2, which binds BAK1 to inhibit complex formation
16 with FLS2 prior to ligand perception [22]. Others, such as the RAF-like kinase EDR1, interact
17 with downstream MEK4 and MEK5 and negatively regulate MEK protein levels through an
18 unidentified process [51]. MKKK7 likely acts at the level of the FLS2 receptor complex, as it
19 co-immunoprecipitates with FLS2 and negatively regulates flg22-induced MAPK activation
20 and downstream *WRKY29* and *FRK1* expression.

21 Interaction of MKKK7 with FLS2 suggests several possible modes of action for attenuation
22 of FLS2 output. It may well be that MKKK7 is competing for FLS2 binding with a positively
23 acting MKKK, such as MEKK1, which in response to flg22 perception activates MPK6
24 through phosphorylation of MEK4 and MEK5 [18]. However, direct binding of other MKKKs
25 to FLS2 has not been reported and several MAPKKs may be regulating flg22 signaling in
26 *Arabidopsis* upstream of the MKK4/MKK5-MPK3/MPK6 cascade (Asai et al.,2002; Suarez-
27 Rodriguez et al.,2007). We also show that in addition to the MAPK branch of PTI signaling,
28 MKKK7 negatively regulates ROS production, which is independent of MAPK activation [44].
29 It is therefore not likely that competition for FLS2 binding with another MKKKs is the only
30 mode of negative regulation. MKKK7 but may act to stabilize protein-protein interaction
31 between FLS2 and another negative regulator, or could affect protein phosphorylation at the
32 level of FLS2 complex or immediate downstream receptor like cytosolic kinases (RLCK)
33 such as BIK1 or one of three related PBLs involved in ROS burst. Since BIK1 and PBL1 are
34 not required for flg22-induced MAPK activation [52], addressing this question requires
35 further in depth analysis of FLS2 complex formation and flg22-induced protein
36 phosphorylation in *mkkk7* mutants.

37

1 **Methods**

2

3 **Plant material**

4 All mutant and transgenic lines used in this study were in the background of *Arabidopsis*
5 *thaliana* accession Columbia (Col-0). The loss-of function T-DNA insertion line *mkkk7*
6 (SALK_133360) was generated by SIGnAL and obtained from the European *Arabidopsis*
7 Stock Centre (NASC) in Nottingham, UK. Plants were grown on soil or on Murashine and
8 Skoog (MS) salt medium (Duchefa) with 1% sucrose and 1% agar. The mutant line *mkkk7*
9 was backcrossed to Col-0 wild-type and genotyped using gene specific primers. All lines
10 were grown under normal long-day growth conditions at 20-22°C and after 4 weeks leaf
11 material was harvested and gDNA was isolated. The position of the insertion was confirmed
12 by genotyping using PCR with gene-specific primers for *MKkk7* 5'-
13 GCAGGATTTTTGTTGTTGTCC-3' and 5'-AATCATTTCTTGGGGTGGATC-3' and 5'-
14 TGGTTCACGTAGTGGGCCATCG-3' for the left border of the T-DNA.

15

16 **RNA extraction and qRT-PCR analyses**

17 Material for RNA analysis was frozen in liquid nitrogen and stored at -80°C. For defense
18 gene analysis duplicate sets of tissue was induced at set time points 0, 1, 2, 3, 4 h after
19 induction with 10 µM of flg22. Tissue was ground in liquid nitrogen followed by extractions
20 using TRIzol reagent (Invitrogen, Carlsbad, CA). Total RNA extractions for RT-PCR and
21 qRT-PCR were performed as described in Menke et al. (2004). cDNA was synthesized from
22 1µg of total RNA using SuperScript II reverse transcriptase (Invitrogen). All RT-PCR
23 reactions were performed under the following conditions: 94°C for 3 min, 26 cycles (94°C for
24 30 sec, 60°C for 30 sec, 72°C for 1 min), and a final extension at 72°C for 5 min. qRT-PCR
25 was performed using the SYBR Green protocol (Applied
26 Biosystems <http://www.appliedbiosystems.com>). Primers used are listed in Appendix Table
27 S1. Each marker gene was normalized to the internal reference gene *At2g29550* (*TUB7*)
28 and plotted relative to the Col-0 mock expression level.

29

30 **SDS-PAGE and MAP kinase assay**

31 Leaf material of 4 week old seedlings was cut into 0.5 cm thin strips and floated in 1 ml of
32 water in a single well of a 24 well plate to recover from wounding stress. After 20-24 h, time-
33 course inductions were done with the synthetic peptide flg22 (Sigma Genosys) at t=0, 5, 10,
34 30 and 60 min. The material was frozen in liquid nitrogen and stored in -80°C. Protein
35 extractions and SDS-PAGE were performed as described in [49]. Equal loading was
36 confirmed by Ponceau S staining and membranes were rinsed in TBS with Tween20
37 (TBST), blocked for 1 h in TBST with 5% nonfat milk powder and incubated overnight at 4°C

1 with polyclonal primary rabbit antibodies raised against MPK3 (a-C-3, 7.5 µg/mL) or MPK6
2 (a-N-6, 5 µg/mL) [49] diluted in TBST solution with 3% BSA (Sigma). Membranes were
3 rinsed 4 times in TBST before incubation with the secondary HRP-conjugated anti-rabbit
4 antibody (1:2000, Cell Signaling). As a loading control, membranes were incubated with α-
5 Actin Mouse IgG, clone C4 antibody (1:1000, ICN), followed by incubation with the
6 secondary antibody anti-mouse-HRP conjugated (1:5000, Novagen). MAP kinase activity
7 was detected using anti-phospho-p44p44/42 MAPK (T202/Y204) primary antibody (1:750,
8 Cell Signaling Technology) in TBST with 3% BSA at 4°C for 16-20 h. Blots were washed as
9 described above after which incubation was continued with a 2 h incubation with anti-rabbit-
10 HRP conjugated secondary antibody (1:2500, Cell Signaling Technology). Antigen-antibody
11 complexes were visualized using chemiluminescence detection with ECL Western Blotting
12 Detection Kit (GE Healthcare) according to the manufacturer's instructions before exposure
13 to film (Kodak).

14

15 **Mesophyll Protoplast Assay**

16 To study transient gene expression, *Arabidopsis* plants were grown in short-day growth
17 conditions. Mesophyll protoplast isolation and transfections of plasmid DNA was conducted
18 as described [53]. To study early transcription responses, three plasmids expressing a
19 regulatory effector, a specific reporter and a transfection control reporter were transfected at
20 the ratio of 4:3:1. Ten µM of the synthetic peptide flg22 was added after 16h incubation of
21 protoplasts at 22°C. We used the promoters of transcription factor WRKY29 and receptor-like
22 kinase FRK1 fused to the firefly luciferase reporter (fLUC) reporter [18] and transiently
23 expressed these constructs in mesophyll protoplasts from Col-0 or *mkkk7* plants. The
24 relative fLUC reporter activity of the defense responsive genes was measured against the
25 rLUC activity using the Dual Luciferase reporter assay system kit (Promega, Madison, USA)
26 according to the manufacturer's instructions. The LUC activity was measured using the TD-
27 20/20 Glomax luminometer (Promega). All fLUC activity was normalized to the non-treated
28 wild type. Constructs used to test PTI in protoplasts are listed in Appendix Table S2 and S3.

29

30 **Generation of transgenic plants**

31 Different promoters were used to study the expression of the *MKKK7* gene (Appendix Table
32 S3). The MultiSite Gateway manufacturer's protocol was used to design primers to clone
33 different promoters in BOX1 entry clone. The 35S promoter, *pG1090:XVE* and *pMKKK7*
34 were cloned in BOX1. *pG1090:XVE* is an estrogen receptor-based chemical inducible
35 system [43] to generate transgenic plants. The second entry clone BOX2 consisted either of
36 the gDNA or the cDNA sequence of *MKKK7*. Selected Serine residues in MKKK7 were
37 mutated according to the manufacturer's instructions for the Stratagene quick change

1 mutagenesis kit. S⁴⁵² and S⁸⁵⁴ were both changed to A (a non-phosphorylatable version) and
2 to D (a phospho-mimic version). BOX3 of the gateway system either had the marker GFP or
3 NOS terminator. The integrity and sequence of all entry clones was confirmed by
4 sequencing. The correct entry clones were combined to one construct (LR reaction). These
5 final constructs were confirmed by restriction digestion. Primers used for PCR amplification
6 for the MultiSite Gateway cloning and for the quick change mutagenesis are listed in
7 Appendix Table S1. Transgenic plants were generated using *Agrobacterium tumefaciens*
8 strain C58. All constructs were transformed into *Arabidopsis* mutant *mkkk7* and Col-0 using
9 the floral dipping method. Transformants were selected on ½ MS agar medium containing
10 40 µg/ml Norf, 35S:*MKkk7-GFP* and amino acid substituted derivative overexpressor
11 constructs were used in the mesophyll protoplast system to study gene transcription
12

13 **Protein extraction and co-immunoprecipitation assays**

14 *Arabidopsis* seedlings expressing FLS2-GFP or the plasma membrane addressed GFP
15 (Lit6b-GFP) were grown axenically for 2 weeks in liquid ½ MS supplemented with 1%
16 sucrose under short day conditions. Elicitation with 10µM flg22 was performed in ½ MS (1%
17 sucrose) for 20 minutes prior storage at -80°C. Ten grams of fresh material per condition
18 were ground in liquid nitrogen using a mortar and pestle. Protein extraction buffer (50 mM
19 MES, pH 6.5, 150 mM NaCl, 10 % glycerol, 5 mM DTT, 0.5 % [w/v] polyvinylpyrrolidone, 1%
20 [v/v] P9599 Protease Inhibitor Cocktail (Sigma-Aldrich), 2% [v/v] for each phosphatases
21 inhibitor cocktail 2 and 3 (Sigma-Aldrich), 100 µM phenylmethylsulphonyl fluoride and 1 %
22 [v/v] IGEPAL CA-630 (Sigma-Aldrich)) was added at 4 mL per gram of tissue powder.
23 Samples were incubated at 4 °C for 30 min and clarified by a 20-min centrifugation at 13,000
24 rpm at 4 °C. Supernatants were incubated for 2 h at 4 °C with 250 µL of anti-GFP magnetic
25 beads (Miltenyi Biotec). Following incubation, magnetic beads were retained using a
26 magnetic stand (Miltenyi Biotec) and washed twice with 250 µL of modified extraction buffer
27 (50 mM MES, pH 6.5, 150 mM NaCl, 10 % glycerol, 0.5% [v/v] IGEPAL CA-630) before
28 eluting proteins by adding 60 µL of boiling hot SDS buffer. Co-immunoprecipitation of FLS2
29 and YFP-MKkk7 were performed as described previously by Schwessinger et al., [8]
30 starting from one gram of fresh tissues per condition.
31

32 **IP-MS Proteomics**

33 Proteins were separated by SDS-PAGE on 10% acrylamide/bis-acrylamide gels. After
34 staining with SimplyBlue™ stain (Invitrogen), proteins were digested by trypsin as described
35 previously [54]. LC-MS/MS analysis was performed using a LTQ-Orbitrap mass
36 spectrometer (Thermo Scientific) and a nanoflow-HPLC system (nanoAcquity; Waters) as
37 described previously [54]. The entire TAIR10 database was searched using Mascot (v 2.3,

1 Matrix Science) search engine with the inclusion of common contaminants sequences such
2 as keratins and trypsin. Precursor and fragment mass tolerances were set for 10 ppm and
3 0.8 Da respectively. Allowed static modification was carbamidomethylation of Cys residues
4 and allowed variable modification was oxidation of Met. Trypsin was used to generate
5 peptides and two missed tryptic cleavages were allowed in the search. Scaffold (v 4.0;
6 Proteome Software), implementation of Peptide Prophet algorithm, was used to validate
7 peptide and protein hits identification with acceptance thresholds set to 95% and 99%
8 respectively and requirement of at least two unique peptide hits per protein Co-
9 immunopurifications and MS/MS analyses of un-elicited, flg22-elicited and Lti6b-GFP control
10 were performed in three independent replicates. The mass spectrometry proteomics data
11 have been deposited to the ProteomeXchange Consortium [55] via the PRIDE partner
12 repository with the dataset identifier PXD003189 and 10.6019/PXD003189

13

14 **ROS assay**

15 Twenty-four leaf disks of 4-5 weeks old plants were collected using a 8 mm cork borer and
16 floated overnight in sterile water containing 2 μ M estradiol. The next day the solution was
17 replaced with 17mg/ml luminol, 10mg/ml horseradish peroxidase and 100 nM flg22 and
18 luminescence was recorded with a CCD camera (Photek) as previously described [56].

19

20 **Sample preparation for Phospho-SRM mass spectrometry**

21 Metabolic labeling of cell cultures and seedlings was described previously and resulted in
22 nearly complete (>99%) labeling [23, 57]. Cultured cells were treated and proteins extracted
23 as described in [16]. Seedlings were grown in liquid culture for 9-10 days starting from 1000
24 seeds per 50 ml of $\frac{1}{2}$ MS culture medium. 15 N labeled Col-0 seedlings were grown in 15 N $\frac{1}{2}$
25 MS medium and started from 15 N labeled seeds obtained from hydroponically grown plants.
26 Sample preparation started from 3 mg of total protein extract (determined using the Bradford
27 assay) dissolved in ammonium bicarbonate buffer containing 8 M urea. First, the protein
28 extracts were reduced with 5 mM Tris (2-carboxyethyl) phosphine (TCEP) for 30 min at 30°C
29 with gentle shaking, followed by alkylation of cysteine residues with 40mM iodoacetamide at
30 room temperature for 1 hour. Subsequently the samples were diluted to a final concentration
31 of 1.6 M urea with 50mM ammonium bicarbonate and digested over night with trypsin
32 (Promega; 1:100 enzyme to substrate ratio). Peptide digests were purified using C18
33 SepPak columns as described before [58]. Phosphopeptides were enriched using titanium
34 dioxide (TiO_2 , GL Science) with Phthalic acid as a modifier as describe before [59].
35 Phosphopeptides were eluted by a pH-shift to 10.5 and immediately purified using C18
36 microspin columns (The Nest Group Inc., 5 – 60 μ g loading capacity). After purification all

1 samples were dried in a speedvac, stored at -80°C and re-suspended in 0.1% formic acid
2 (FA) just before the mass spectrometric measurement.

4 **SRM mass spectrometry**

5 SRM measurements were performed as described by Ludwig et al., (2012) with minor
6 changes. Briefly, analysis was carried out on a TSQ Vantage triple quadrupole mass
7 spectrometer (Thermo Fischer Scientific) equipped with a nano-electrospray ion source,
8 coupled to a nano-LC system (Eksigent). Aliquots of phospho-enriched samples were
9 loaded onto a 75 µm x 10 cm fused silica microcapillary reverse phase column, in-house
10 packed with Magic C18 AQ material (200Å pore, 5 µm diameter, Michrom BioResources).
11 For peptide separation a linear 30 min gradient from 2% to 35% solvent B (solvent A: 98%
12 water, 2% acetonitrile, 0.1% formic acid; solvent B: 98% acetonitrile, 2% water, 0.1% formic
13 acid) at 300 nL/min flow rate was applied. For each sample three biological replicates were
14 analyzed. SRM-assays were developed and optimized using light (¹⁴N) crude synthetic
15 phosphopeptides (JPT peptide technologies, Germany). Synthetic phosphopeptide mixes
16 were analyzed first by SRM-triggered MS2 on a triple quadrupole mass spectrometer. The
17 hereby-generated full MS2 spectra were used to identify the 6 most intense transitions per
18 peptide and to determine the peptide retention time relative to a set of retention time
19 reference peptides (iRTs) [60]. For synthetic phosphopeptides that did not trigger an MS2
20 spectrum the 6 most intense transitions were selected from SRM measurements of the
21 complete y- and b-ion series of the doubly and triply charged precursor ions.

23 **SRM Data analysis**

24 The raw data files were imported into the Skyline software package [61]. Confident peptide
25 identification was carried out based on co-elution of light and heavy peptide peaks, iRT
26 information and matching relative transitions intensities between the SRM peak and the
27 library MS2 spectrum (if available). For accurate peptide quantification low quality or
28 interfered transitions were removed manually. The refined dataset can be accessed via
29 [https://daily.panoramaweb.org/labkey/project/Aebersold/ludwig/Mithoe_2014_Arabidopsis_](https://daily.panoramaweb.org/labkey/project/Aebersold/ludwig/Mithoe_2014_Arabidopsis_phospho_SRM/begin.view)
30 [phospho_SRM/begin.view](https://daily.panoramaweb.org/labkey/project/Aebersold/ludwig/Mithoe_2014_Arabidopsis_phospho_SRM/begin.view)). Quantification was based on the integrated peptide peak area,
31 which was calculated by summing all transition areas associated to the light (synthetic spike
32 or endogenous mutant) or heavy peptide (endogenous wildtype), respectively. The statistical
33 significance analysis (student *t*-test) was carried out in Microsoft Excel (Dataset EV2). All
34 SRM assay information and raw data has been deposited to the Panorama Skyline server
35 and can be accessed via:
36 [https://daily.panoramaweb.org/labkey/project/Aebersold/ludwig/Mithoe_2014_Arabidopsis_](https://daily.panoramaweb.org/labkey/project/Aebersold/ludwig/Mithoe_2014_Arabidopsis_phospho_SRM/begin.view)
37 [phospho_SRM/begin.view](https://daily.panoramaweb.org/labkey/project/Aebersold/ludwig/Mithoe_2014_Arabidopsis_phospho_SRM/begin.view)).

1

2 **Pathogen inoculation and analysis of resistance**

3 Plants were individually transplanted into soil and grown for the required amount of time in
4 short day conditions (10 h day; $100 \mu\text{E}\cdot\text{m}^{-2}\cdot\text{s}^{-1}$; 21°C). *P. syringae* pv. *tomato* DC3000 (*Pst*
5 DC3000) was grown overnight at 28°C in Kings B medium supplemented with appropriate
6 antibiotics as described [49]. Cells were harvested by centrifugation (10 min at 4000 rpm)
7 and pellets were resuspended in 10 mM MgSO_4 and diluted to a proper OD_{600} . For spray
8 and dip inoculations, 0.015% (v/v) Silwet L-77 (Van Meeuwen Chemicals, Weesp,
9 Netherlands) was added. For *Pst* DC3000 infiltration assays ($\text{OD}_{600}=0.0005$) leaves of 4-
10 week-old plants were pressure infiltrated using a needleless syringe. After inoculation plants
11 were grown at short day conditions with high humidity. To quantify pathogen growth after
12 inoculation, 2 leaf discs from 2 leaves per plant were harvested ($n=5$) and ground in 10 mM
13 MgCl_2 . Dilutions were plated on Kings B medium with 50 mg/mL of rifampicin and incubated
14 at 28°C for 48 h, after which the number of colonies was determined. For *Pst* DC3000 dip
15 inoculation ($\text{OD}_{600}=0.025$) leaves were dipped in a bacterial suspension including Silwet L-
16 77 for 2 seconds. After inoculation plants were grown at short day conditions with high
17 humidity. Two to four days after inoculation the disease index was determined by scoring
18 each leaf diseased or not diseased resulting in a percentage of diseased leaves per plant
19 ($n=20$). Inducible transgenic lines carrying *MKKK7^{AA}* and *MKKK7^{DD}* were sprayed with $5 \mu\text{M}$
20 estradiol solution 24 h prior to inoculation.

21

22 **Acknowledgements**

23 Authors would like to thank Alberto Macho, Jacqueline Monaghan and Sophien
24 Kamoun for critically reading the manuscript. We would like to acknowledge Mariette
25 Matondo and Alessio Maiolica for their support and maintenance of the mass
26 spectrometers at ETH and Alex Jones for support and maintenance of the mass
27 spectrometers at TSL and Cyril Zipfel and Yasu Kadota for setting up co-IPs at TSL.
28 Authors would like to thank Eric Talevich for bioinformatics help and Katrin Werler for
29 practical assistance. We would also like to acknowledge Frits Kindt and Ronald Leito
30 for photography and help in preparing figures. Research was funded through Casimir
31 fellowship (NWO, the Netherlands) to SCM and partly financed through Gatsby
32 Charitable foundation.

33

1 **Author contributions:** SCM, CL, MJCP, MC, AC, MM, PD, JS and FLHM performed
2 experiments; SCM, CL, SR, CP, RA and FLHM conceived experiments and analyzed data
3 and SCM, CL and FLHM wrote manuscript.

4
5 **Conflict of interest:** Authors declare no conflict of interest
6

7
8 **References**
9

- 10 1. Nicaise V, Roux M, Zipfel C (2009) Recent advances in PAMP-triggered immunity
11 against bacteria: pattern recognition receptors watch over and raise the alarm. *Plant*
12 *Physiol* **150**: 1638-47
- 13 2. Gomez-Gomez L, Boller T (2000) FLS2: an LRR receptor-like kinase involved in
14 the perception of the bacterial elicitor flagellin in Arabidopsis. *Mol Cell* **5**: 1003-11
- 15 3. Chinchilla D, Zipfel C, Robatzek S, Kemmerling B, Nurnberger T, Jones JDG, Felix
16 G, Boller T (2007) A flagellin-induced complex of the receptor FLS2 and BAK1 initiates
17 plant defence. *Nature* **448**: 497-500
- 18 4. Sun Y, Li L, Macho AP, Han Z, Hu Z, Zipfel C, Zhou JM, Chai J (2013) Structural
19 basis for flg22-induced activation of the Arabidopsis FLS2-BAK1 immune complex.
20 *Science* **342**: 624-8
- 21 5. Tena G, Boudsocq M, Sheen J (2011) Protein kinase signaling networks in plant
22 innate immunity. *Curr Opin Plant Biol* **14**: 519-29
- 23 6. Macho AP, Zipfel C (2014) Plant PRRs and the Activation of Innate Immune
24 Signaling. *Mol Cell* **54**: 263-272
- 25 7. Rasmussen MW, Roux M, Petersen M, Mundy J (2012) MAP Kinase Cascades in
26 Arabidopsis Innate Immunity. *Frontiers in plant science* **3**: 169
- 27 8. Schwessinger B, Ronald PC (2012) Plant innate immunity: perception of
28 conserved microbial signatures. *Annu Rev Plant Biol* **63**: 451-82
- 29 9. Cui H, Xiang T, Zhou JM (2009) Plant immunity: a lesson from pathogenic
30 bacterial effector proteins. *Cell Microbiol* **11**: 1453-61
- 31 10. Schulze-Lefert P, Panstruga R (2003) Establishment of biotrophy by parasitic
32 fungi and reprogramming of host cells for disease resistance. *Annu Rev Phytopathol* **41**:
33 641-67
- 34 11. Jones JDG, Dangl JL (2006) The plant immune system. *Nature* **444**: 323-329

- 1 12. Boller T, He SY (2009) Innate Immunity in Plants: An Arms Race Between
2 Pattern Recognition Receptors in Plants and Effectors in Microbial Pathogens. *Science*
3 **324**: 742-744
- 4 13. Thomma BP, Nurnberger T, Joosten MH (2011) Of PAMPs and effectors: the
5 blurred PTI-ETI dichotomy. *Plant Cell***23**: 4-15
- 6 14. Rodriguez MC, Petersen M, Mundy J (2010) Mitogen-activated protein kinase
7 signaling in plants. *Annu Rev Plant Biol* **61**: 621-49
- 8 15. Pitzschke A, Schikora A, Hirt H (2009) MAPK cascade signalling networks in
9 plant defence. *Curr Opin Plant Biol* **12**: 421-6
- 10 16. Mithoe SC, Boersema PJ, Berke L, Snel B, Heck AJ, Menke FL (2012) Targeted
11 quantitative phosphoproteomics approach for the detection of phospho-tyrosine
12 signaling in plants. *J Proteome Res* **11**: 438-448
- 13 17. Suarez-Rodriguez MC, Adams-Phillips L, Liu Y, Wang H, Su S-H, Jester PJ, Zhang S,
14 Bent AF, Krysan PJ (2007) MEKK1 Is Required for flg22-Induced MPK4 Activation in
15 Arabidopsis Plants. *Plant Physiology* **143**: 661-669
- 16 18. Asai T, Tena G, Plotnikova J, Willmann MR, Chiu WL, Gomez-Gomez L, Boller T,
17 Ausubel FM, Sheen J (2002) MAP kinase signalling cascade in Arabidopsis innate
18 immunity. *Nature* **415**: 977-83
- 19 19. Kadota Y, Sklenar J, Derbyshire P, Stransfeld L, Asai S, Ntoukakis V, Jones JD,
20 Shirasu K, Menke F, Jones A, *et al.* (2014) Direct regulation of the NADPH oxidase
21 RBOHD by the PRR-associated kinase BIK1 during plant immunity. *Mol Cell* **54**: 43-55
- 22 20. Li L, Li M, Yu L, Zhou Z, Liang X, Liu Z, Cai G, Gao L, Zhang X, Wang Y, *et al.* (2014)
23 The FLS2-Associated Kinase BIK1 Directly Phosphorylates the NADPH Oxidase RbohD
24 to Control Plant Immunity. *Cell Host Microbe* **15**: 329-38
- 25 21. Segonzac C, Macho AP, Sanmartin M, Ntoukakis V, Sanchez-Serrano JJ, Zipfel C
26 (2014) Negative control of BAK1 by protein phosphatase 2A during plant innate
27 immunity. *EMBO J* **33**: 2069-79
- 28 22. Halter T, Imkampe J, Mazzotta S, Wierzba M, Postel S, Bucherl C, Kiefer C, Stahl M,
29 Chinchilla D, Wang X, *et al.* (2014) The Leucine-Rich Repeat Receptor Kinase BIR2 Is a
30 Negative Regulator of BAK1 in Plant Immunity. *Curr Biol* **24**: 134-43
- 31 23. Benschop JJ, Mohammed S, O'Flaherty M, Heck AJR, Slijper M, Menke FLH (2007)
32 Quantitative Phosphoproteomics of Early Elicitor Signaling in Arabidopsis. *Mol Cell*
33 *Proteomics* **6**: 1198-1214

- 1 24. Nuhse TS, Bottrill AR, Jones AME, Peck SC (2007) Quantitative
2 phosphoproteomic analysis of plasma membrane proteins reveals regulatory
3 mechanisms of plant innate immune responses. *The Plant Journal* **51**: 931-940
- 4 25. Nuhse TS, Stensballe A, Jensen ON, Peck SC (2004) Phosphoproteomics of the
5 Arabidopsis plasma membrane and a new phosphorylation site database. *Plant Cell* **16**:
6 2394-405
- 7 26. Zhang J, Li W, Xiang T, Liu Z, Laluk K, Ding X, Zou Y, Gao M, Zhang X, Chen S, *et al.*
8 (2010) Receptor-like cytoplasmic kinases integrate signaling from multiple plant
9 immune receptors and are targeted by a *Pseudomonas syringae* effector. *Cell Host*
10 *Microbe* **7**: 290-301
- 11 27. Boudsocq M, Willmann MR, McCormack M, Lee H, Shan L, He P, Bush J, Cheng SH,
12 Sheen J (2010) Differential innate immune signalling via Ca(2+) sensor protein kinases.
13 *Nature* **464**: 418-22
- 14 28. Chung EH, El-Kasmi F, He Y, Loehr A, Dangl JL (2014) A Plant Phosphoswitch
15 Platform Repeatedly Targeted by Type III Effector Proteins Regulates the Output of
16 Both Tiers of Plant Immune Receptors. *Cell Host Microbe* **16**: 484-94
- 17 29. Champion A, Picaud A, Henry Y (2004) Reassessing the MAP3K and MAP4K
18 relationships. *Trends in Plant Science* **9**: 123-129
- 19 30. Jin H, Axtell MJ, Dahlbeck D, Ekwenna O, Zhang S, Staskawicz B, Baker B (2002)
20 NPK1, an MEKK1-like mitogen-activated protein kinase kinase kinase, regulates innate
21 immunity and development in plants. *Dev Cell* **3**: 291-7
- 22 31. Frye CA, Tang D, Innes RW (2001) Negative regulation of defense responses in
23 plants by a conserved MAPKK kinase. *Proc Natl Acad Sci U S A* **98**: 373-8
- 24 32. Ichimura K, Shinozaki K, Tena G, Sheen J, Henry Y, Champion A, Kreis M, Zhang S,
25 Hirt H, Wilson C, *et al.* (2002) Mitogen-activated protein kinase cascades in plants: a
26 new nomenclature. *Trends in Plant Science* **7**: 301-308
- 27 33. Gao M, Liu J, Bi D, Zhang Z, Cheng F, Chen S, Zhang Y (2008) MEKK1,
28 MKK1/MKK2 and MPK4 function together in a mitogen-activated protein kinase
29 cascade to regulate innate immunity in plants. *Cell Res* **18**: 1190-8
- 30 34. Nishihama R, Ishikawa M, Araki S, Soyano T, Asada T, Machida Y (2001) The
31 NPK1 mitogen-activated protein kinase kinase kinase is a regulator of cell-plate
32 formation in plant cytokinesis. *Genes Dev* **15**: 352-63

- 1 35. del Pozo O, Pedley KF, Martin GB (2004) MAPKKK α is a positive regulator of
2 cell death associated with both plant immunity and disease. *EMBO J* **23**: 3072-82
- 3 36. Melech-Bonfil S, Sessa G (2010) Tomato MAPKKK ϵ is a positive regulator
4 of cell-death signaling networks associated with plant immunity. *Plant J* **64**: 379-91
- 5 37. King SRF, McLellan H, Boevink PC, Armstrong MR, Bukharova T, Sukarta O, Win J,
6 Kamoun S, Birch PRJ, Banfield MJ (2014) Phytophthora infestans RXLR Effector PexRD2
7 Interacts with Host MAPKKK ϵ to Suppress Plant Immune Signaling. *The Plant Cell*
8 *Online*
- 9 38. Cutler SR, Ehrhardt DW, Griffitts JS, Somerville CR (2000) Random GFP::cDNA
10 fusions enable visualization of subcellular structures in cells of Arabidopsis at a high
11 frequency. *Proc Natl Acad Sci U S A* **97**: 3718-23
- 12 39. Chaiwongsar S, Otegui MS, Jester PJ, Monson SS, Krysan PJ (2006) The protein
13 kinase genes MAP3K epsilon 1 and MAP3K epsilon 2 are required for pollen viability in
14 Arabidopsis thaliana. *Plant J* **48**: 193-205
- 15 40. Reiland S, Messerli G, Baerenfaller K, Gerrits B, Endler A, Grossmann J, Gruissem
16 W, Baginsky S (2009) Large-scale Arabidopsis phosphoproteome profiling reveals novel
17 chloroplast kinase substrates and phosphorylation networks. *Plant Physiol* **150**: 889-
18 903
- 19 41. Nuhse TS, Peck SC, Hirt H, Boller T (2000) Microbial elicitors induce activation
20 and dual phosphorylation of the Arabidopsis thaliana MAPK 6. *The Journal of biological*
21 *chemistry* **275**: 7521-6
- 22 42. Sours KM, Xiao Y, Ahn NG (2014) Extracellular-regulated kinase 2 is activated by
23 the enhancement of hinge flexibility. *J Mol Biol* **426**: 1925-35
- 24 43. Zuo J, Niu QW, Chua NH (2000) Technical advance: An estrogen receptor-based
25 transactivator XVE mediates highly inducible gene expression in transgenic plants.
26 *Plant J* **24**: 265-73
- 27 44. Xu J, Xie J, Yan C, Zou X, Ren D, Zhang S (2013) A chemical genetic approach
28 demonstrates that MPK3/MPK6 activation and NADPH oxidase-mediated oxidative
29 burst are two independent signaling events in plant immunity. *Plant J*
- 30 45. Oh CS, Pedley KF, Martin GB (2010) Tomato 14-3-3 protein 7 positively regulates
31 immunity-associated programmed cell death by enhancing protein abundance and
32 signaling ability of MAPKKK { α }. *Plant Cell* **22**: 260-72

- 1 46. Zhang J, Shao F, Li Y, Cui H, Chen L, Li H, Zou Y, Long C, Lan L, Chai J, *et al.* (2007)
2 A *Pseudomonas syringae* effector inactivates MAPKs to suppress PAMP-induced
3 immunity in plants. *Cell Host Microbe* **1**: 175-85
- 4 47. Anderson JC, Bartels S, Besteiro MAG, Shahollari B, Ulm R, Peck SC (2011)
5 Arabidopsis MAP Kinase Phosphatase 1 (AtMKP1) negatively regulates MPK6-mediated
6 PAMP responses and resistance against bacteria. *The Plant Journal* **67**: 258-268
- 7 48. Bartels S, Anderson JC, Gonzalez Besteiro MA, Carreri A, Hirt H, Buchala A,
8 Metraux JP, Peck SC, Ulm R (2009) MAP kinase phosphatase1 and protein tyrosine
9 phosphatase1 are repressors of salicylic acid synthesis and SNC1-mediated responses in
10 Arabidopsis. *Plant Cell* **21**: 2884-97
- 11 49. Menke FL, van Pelt JA, Pieterse CM, Klessig DF (2004) Silencing of the mitogen-
12 activated protein kinase MPK6 compromises disease resistance in Arabidopsis. *Plant*
13 *Cell* **16**: 897-907
- 14 50. Beckers GJM, Jaskiewicz M, Liu Y, Underwood WR, He SY, Zhang S, Conrath U
15 (2009) Mitogen-Activated Protein Kinases 3 and 6 Are Required for Full Priming of
16 Stress Responses in Arabidopsis thaliana. *Plant Cell* **21**: 944-953
- 17 51. Zhao C, Nie H, Shen Q, Zhang S, Lukowitz W, Tang D (2014) EDR1 Physically
18 Interacts with MKK4/MKK5 and Negatively Regulates a MAP Kinase Cascade to
19 Modulate Plant Innate Immunity. *PLoS Genet* **10**: e1004389
- 20 52. Ranf S, Eschen-Lippold L, Frohlich K, Westphal L, Scheel D, Lee J (2014) Microbe-
21 associated molecular pattern-induced calcium signaling requires the receptor-like
22 cytoplasmic kinases, PBL1 and BIK1. *BMC plant biology* **14**: 374
- 23 53. Yoo SD, Cho YH, Sheen J (2007) Arabidopsis mesophyll protoplasts: a versatile
24 cell system for transient gene expression analysis. *Nat Protoc* **2**: 1565-72
- 25 54. Ntoukakis V, Mucyn TS, Gimenez-Ibanez S, Chapman HC, Gutierrez JR, Balmuth
26 AL, Jones AM, Rathjen JP (2009) Host inhibition of a bacterial virulence effector triggers
27 immunity to infection. *Science* **324**: 784-7
- 28 55. Vizcaino JA, Deutsch EW, Wang R, Csordas A, Reisinger F, Rios D, Dianas JA, Sun
29 Z, Farrah T, Bandeira N, *et al.* (2014) ProteomeXchange provides globally coordinated
30 proteomics data submission and dissemination. *Nat Biotechnol* **32**: 223-6
- 31 56. Schwessinger B, Roux M, Kadota Y, Ntoukakis V, Sklenar J, Jones A, Zipfel C
32 (2011) Phosphorylation-Dependent Differential Regulation of Plant Growth, Cell Death,

- 1 and Innate Immunity by the Regulatory Receptor-Like Kinase BAK1. *PLoS Genet* **7**:
2 e1002046
- 3 57. Zhang H, Zhou H, Berke L, Heck AJ, Mohammed S, Scheres B, Menke FL (2013)
4 Quantitative phosphoproteomics after auxin-stimulated lateral root induction identifies
5 an SNX1 protein phosphorylation site required for growth. *Mol Cell Proteomics* **12**:
6 1158-69
- 7 58. Ludwig C, Claassen M, Schmidt A, Aebersold R (2012) Estimation of absolute
8 protein quantities of unlabeled samples by selected reaction monitoring mass
9 spectrometry. *Mol Cell Proteomics* **11**: M111 013987
- 10 59. Bodenmiller B, Wanka S, Kraft C, Urban J, Campbell D, Pedrioli PG, Gerrits B,
11 Picotti P, Lam H, Vitek O, *et al.* (2010) Phosphoproteomic analysis reveals
12 interconnected system-wide responses to perturbations of kinases and phosphatases in
13 yeast. *Sci Signal* **3**: rs4
- 14 60. Escher C, Reiter L, MacLean B, Ossola R, Herzog F, Chilton J, MacCoss MJ, Rinner
15 O (2012) Using iRT, a normalized retention time for more targeted measurement of
16 peptides. *Proteomics* **12**: 1111-21
- 17 61. MacLean B, Tomazela DM, Shulman N, Chambers M, Finney GL, Frewen B, Kern R,
18 Tabb DL, Liebler DC, MacCoss MJ (2010) Skyline: an open source document editor for
19 creating and analyzing targeted proteomics experiments. *Bioinformatics* **26**: 966-8
- 20 62. Albrecht C, Boutrot F, Segonzac C, Schwessinger B, Gimenez-Ibanez S, Chinchilla
21 D, Rathjen JP, de Vries SC, Zipfel C (2012) Brassinosteroids inhibit pathogen-associated
22 molecular pattern-triggered immune signaling independent of the receptor kinase
23 BAK1. *Proc Natl Acad Sci U S A* **109**: 303-8

24
25

26 **Figure legends**

27

28 **Figure 1. Flagellin receptor FLS2 co-immunoprecipitates with MKKK7.**
29 Immunoprecipitation was performed with GFP-binding protein immobilized on magnetic
30 beads using extracts of *Arabidopsis* seedlings, expressing either YFP-MKKK7 or Lti6B.
31 Seedlings were treated with 1 μ M flg22 for the indicated time. YFP-MKKK7 and Lti6B-GFP
32 were detected with an anti-GFP antibody while FLS2 was detected with an FLS-specific
33 antibody. Upper panel shows (co)-immunoprecipitated proteins, lower panel shows input
34 levels of protein. Arrowheads indicate the position of proteins of interest.

1
2
3
4
5
6
7
8
9
10
11
12
13
14
15
16
17
18
19
20
21
22
23
24
25
26
27
28
29
30
31
32
33
34
35
36
37

Figure 2. Transient phosphorylation of MKKK7 and other MAP kinases upon flg22 treatment. Application of selected reaction monitoring (SRM) mass spectrometry to quantify phosphorylated peptides in cell extracts treated with 1 μ M flg22. Bars represent the mean ratio of endogenous phosphopeptide versus spiked-in synthetic phosphopeptide normalized to t = 0 with error bars \pm SEM ($n=3$). Asterisks indicate significant difference level compared to t = 0 (student t -test, * >0.05 , ** >0.01 and *** >0.001). The color of each bar corresponds to the different time points (0 minutes = dark blue, 5 minutes = red, 10 minutes = green, 20 minutes = purple, 30 minutes = light blue). Above each graph is the protein name and the phosphorylated residue (in brackets) is indicated and below the corresponding phosphopeptide is shown with the Serine (S), Threonine (T) or Tyrosine (Y) phosphorylation site indicated by "[+80]".

Figure 3. Flg22-induced MAPK phosphorylation is enhanced in the *mkkk7* mutant. A) Immunoblot analyses showing MAPK phosphorylation after flg22 induction in Col-0 and in *mkkk7*. Protein extracts were made from seedlings treated with 1 μ M flg22 and samples were taken at t=0, 10 and 30 min post induction. The p44/42 antibody was used to detect phosphorylated MAPKs. Position of the individual phosphorylated MAPKs is indicated at the right. Equal loading of proteins is shown with an α -Actin antibody as a loading control (bottom panel). Three biological replicates were done with identical results **B)** MPK6 phosphorylation is specifically enhanced in *mkkk7*. Comparison of phosphopeptide abundances from selected MAP kinases in Col-0 (blue) and *mkkk7* (red) seedlings at t = 0 min and t = 10 min after 1 μ M flagellin treatment by selected reaction monitoring (SRM) mass spectrometry. Phosphopeptide corresponding to MKKK7 are only detectable in Col-0 seedlings and are non-detectable (ND) in *mkkk7*. Bars represent means of measured peptide areas (sum of all transition areas) for three biological replicates, with error bars \pm SEM ($n=3$). Asterisks indicate significant difference between Col-0 and *mkkk7* at individual time points (student t -test, * >0.05 , ** >0.01 and *** >0.001). ND indicates integration of an area without transitions significantly above background. Above each graph the protein name and the phosphorylated residue (in brackets) is indicated as well as the corresponding phosphopeptide sequence. Serine (S), Threonine (T) or Tyrosine (Y) phosphorylation is indicated by "[+80]".

Figure 4. Flg22-induced defense gene expression is enhanced in *mkkk7*. A) Transient expression analysis in *Arabidopsis* mesophyll protoplasts shows enhanced defense gene expression in *mkkk7* protoplasts after flg22 treatment. Protoplasts were isolated from 4 week old plants and transfected with *pWKRY29:fluc* (*WRKY29*) or *pFRK1:fluc*(*FRK1*)

1 constructs together with *35S:rLUC*, as indicated in the graph. Protoplasts were treated for 4
2 hrs with 10 μ M flg22 or mock treated as indicated. The horizontal axis indicates the
3 treatment while the vertical axis represents expression levels relative to the mock treated
4 control sample, as fold induction. All measurements were normalized to the *rLUC* activity.
5 Bars represent means \pm STDEV ($n=2$). Experiment was repeated 6 times with similar
6 results. **B)** *WRKY29* transcripts measured by qRT-PCR in flg22 treated leaf material. Leaf
7 strips of Col-0 and *mkkk7* were treated with 1 μ M flg22 for $t=0, 1, 2,$ and 4h. *WRKY29*
8 transcripts were normalized against *Ubiquitin* transcript as described before [62]. Bars
9 represent mean value and error bars show SE ($n=3$). (* $p<0.05$, ** $p<0.01$, student *t*-test). **C)**
10 *FRK1* transcripts measured by qRT-PCR in flg22 treated leaf material. Leaf strips of Col-0
11 and *mkkk7* were treated with 1 μ M flg22 for $t=0, 1, 2,$ and 4h. *FRK1* transcripts were
12 normalized against *Ubiquitin* transcript as described before [62]. Bars represent mean value
13 and error bars show SE ($n=3$). (* $p<0.05$, ** $p<0.01$, student *t*-test). For each qRT-PCR
14 experiments shown in **B)** and **C)** at least 2 biological replicates were done showing the same
15 trend.

16

17 **Figure 5. Phosphorylation of MKKK7 on specific Serine residues is required for**
18 **negative regulation of flg22-induced WRKY29 gene expression.** **A)** Transient co-
19 expression of *MKKK7* in *Arabidopsis* mesophyll protoplasts shows suppression of flg22-
20 induced *WRKY29* gene expression. Protoplasts were transfected with *pWRKY29:fLUC*,
21 *35S:rLUC* and indicated overexpression constructs of *MKKK7* (*OE-MKKK7*, *OE-MKKK7^{AA}* or
22 *OE-MKKK7^{DD}*) as indicated on the horizontal axis. Protoplasts were treated with 10 μ M flg22
23 or mock treated for 4 hrs. All measurements were normalized to the *rLUC* activity and
24 expression is relative to the mock treated control sample, shown as fold induction on the
25 vertical axis. Results shown are means \pm STDEV ($n=2$). At least two biological replicates
26 were done with similar results **B)** Protein structure of *MKKK7* and mutated versions of
27 *MKKK7* with the protein kinase domain shown in yellow and an ARM/HEAT repeat domain
28 shown in blue. The position of the phosphorylated Serine residues is indicated with triangles
29 and bold S below the protein structure. The red triangles indicate phosphorylated Serines
30 that were targeted for mutagenesis or the corresponding phospho-mimic Aspartic acid. Blue
31 triangles indicate the substitution with the non-phosphorylatable amino acid Alanine. Amino
32 acid substitute versions of *MKKK7* are shown below the wild-type. S, Serine; A, Alanine; D,
33 Aspartic acid.

34

35 **Figure 6. MKKK7 negatively regulates basal resistance to virulent bacterial infection.**
36 **A)** Four-week-old seedlings were dipped into a suspension containing virulent *Pst* DC3000
37 and 72 h later the disease symptoms were scored. Data represents mean values \pm SEM

1 ($n=20$;***, $p<0.001$; paired t -test). Three biological experiments were done showing similar
2 results. **B)** Quantification of bacterial growth in *Arabidopsis* lines Col-0, *mkkk7* and
3 p35S:*MKKK7-GFP* in the *mkkk7* background. Four to five-week-old plants were pressure-
4 infiltrated with virulent *Pst* DC3000 and at indicated time points 6 samples were harvested
5 and bacteria re-isolated on selective media. The number of colony forming units (cfu/cm²)
6 was determined at $t=0$, 2 and 3 days post inoculation (dpi). Data represents mean values \pm
7 SEM ($n=6$; **, $p<0.01$; paired t -test). Experiments were done at least twice with similar
8 results. **C)** Disease symptom development in *Pst*-infected lines with estradiol inducible
9 constructs of *ind-MKKK7^{AA}* L8, *ind-MKKK7^{AA}* L10, *ind-MKKK7^{DD}* L1 and *ind-MKKK7^{DD}* L3.
10 Two independent transgenic lines for each construct were grown under short-day conditions
11 and disease symptoms were scored 3 dpi. Data represents mean values \pm SEM ($n=20$; *,
12 $p<0.05$; **, $p<0.01$; paired t -test). The vertical axis represents the percentage disease
13 symptoms. Experiments were done at least twice with similar results.
14

15 **Figure 7. Overexpression of MKKK7^{DD} reduces flg22-induced ROS burst in leaves.**
16 Analysis of reactive oxygen species (ROS) production after treatment with flg22. **A)** Effect of
17 100 nM flg22 treatment on ROS burst measured in 5 week old plants of Col-0 and *mkkk7*. **B)**
18 Effect of 100 nM flg22 treatment on the ROS burst measured in 5 week old plants of Col-0
19 and two independent inducible *MKKK7^{AA}* transgenic lines. **C)** Effect of 100 nM flg22
20 treatment on the ROS burst measured in 5 weeks old plants of Col-0 and two independent
21 inducible *MKKK7^{DD}* transgenic lines. Graphs represent means with error bars \pm SEM ($n=24$).
22 The vertical axis represents the relative increase in ROS production (photon counts) after
23 PAMP treatment. At least three biological replicate experiments were done with similar
24 results.
25

26 Expanded view figure legends

27
28 **Figure EV1. MS/MS spectra of peptides mapped to MKKK7.** LTQ-Orbitrap MS/MS
29 spectra of MKKK7 peptides identified in FLS2-GFP co-immunoprecipitated samples. Peptide
30 sequence and fragmentation pattern are shown above the spectra together with the
31 observed m/z and charge state of the precursor ion.
32

33 **Figure EV2. MKKK7 domain structure and phosphorylated residues.** **A)** Protein
34 structure of MKKK7 with the protein kinase domain shown in yellow and an ARM/HEAT
35 repeat domain shown in blue. The position of the phosphorylated Serine residues (S) is
36 shown with triangles. The green triangles indicate non-differentially phosphorylated sites.
37 The red triangles indicate phosphorylated Serine (pS) sites that were targeted for

1 mutagenesis. **B)** Protein sequence of MKKK7, highlighted in yellow are all (phospho-)
2 peptides measured by mass spectrometry. Highlighted in green are modified residues and
3 the red box around the S residues indicates phosphorylated Serine residues that were
4 targeted for mutagenesis.

5
6 **Figure EV3. Multiple sequence alignment of MKKK7 and related MAP3K.** Amino acid
7 sequences for *Arabidopsis thaliana* MKKK6 (AtMKKK6) and MKKK7 (AtMKKK7),
8 *Arabidopsis lyrata* MKKK7 (AIMKKK7), *Brassica napus* MAP3K epsilon protein kinase 1
9 (BnM3KE1), *Camelina sativa* MAP3K epsilon protein kinase (CsM3KE), *Solanum*
10 *lycopersicum* MAP3K epsilon protein kinase (SIM3KE), *Nicotiana benthamiana* MAP3K
11 epsilon protein kinase (NbM3KE), *Malus domestica* MAP3K epsilon protein kinase
12 (MdM3KE) and *Populus trichocarpa* MAP3K epsilon protein kinase (PtM3KE) were aligned
13 with Clustal Omega (<http://www.ebi.ac.uk/Tools/msa/clustalo/>). Residues phosphorylated in
14 AtMKKK7 are indicated with a red arrow and highlighted in red, conserved residues in other
15 MAP3Ks are highlighted in green. Protein names and Genbank accession numbers are
16 indicated on the left side of the alignments.

17
18 **Figure EV4. MAP kinase activation loop phosphorylation.** **A)** Selected reaction
19 monitoring (SRM) of MPK6 activation loop phosphorylation in response to flg22 stimulation
20 in cultured cells. **B)** SRM of MPK3 activation loop phosphorylation in response to flg22
21 stimulation in cultured cells. Mono and doubly phosphorylated versions of the tryptic MPK
22 activation loop peptides were monitored at 0, 5, 10, 20 and 30 min after stimulation with 1
23 μ M flg22. Sequences are shown on the left, with lower case p indicating phosphorylation of
24 the residue to the right. Left panels show integrated peak area data for three biological
25 replicates (A, B and C). Middle panels show examples of transitions measured for
26 endogenous 15 N labeled peptides. Right panels show examples of total integrated peak area
27 for endogenous 15 N labeled peptides and 14 N labeled synthetic peptides, which were spiked
28 into the samples at a constant amount.

29
30 **Figure EV5. Phosphorylation of MKKK7 on specific Serine residues is required for**
31 **negative regulation of flg22-induced FRK1 gene expression.** Transient co-expression of
32 MKKK7 in *Arabidopsis* mesophyll protoplasts shows suppression of FRK1 gene expression
33 in protoplasts after flg22 treatment. Protoplasts were isolated from four-week-old plants and
34 transfected with *pFRK1::fLUC*, *35S::rLUC* and overexpression constructs of MKKK7 (*OE-*
35 *MKKK7*, *OE-MKKK7^{AA}* or *OE-MKKK7^{DD}*) as indicated on the horizontal axis. Sixteen hours
36 later, protoplasts were treated with 10 μ M flg22 for 4 hrs. All measurements were normalized

1 to the rLUC activity and expression levels were calculated relative to the mock treated
 2 control sample as shown as fold induction represented on the vertical axis.

3
 4 **Figure EV6. MKKK7 negatively regulates basal resistance to virulent bacterial**
 5 **infection. A)** Example of symptom development at 2 dpi in the *p35S:MKKK7-GFP* in *mkkk7*
 6 background as compared to Col-0. Example of symptom development at 2 dpi in *mkkk7* and
 7 *p35S:MKKK7-GFP* in *mkkk7* background. **B)** Overexpression of *MKKK7^{DD}* reduces
 8 resistance to *Pst* infection. Quantification of bacterial growth in Col-0 and two independent
 9 *iMKKK7^{DD}* lines. Four to five-week-old plants were pressure-infiltrated with virulent *Pst*
 10 DC3000 and at 2 dpi leaf disks were harvested and bacteria re-isolated. The number of
 11 colony forming units (cfu/cm²) was determined at t=2 days post inoculation (dpi). Data
 12 represents mean values ± SEM (n=6; *, p<0.05; paired t-test).

13

14

15 **Table I FLS2-GFP co-immunoprecipitates with MKKK7.**

Protein name	Protein accession numbers	Peptide sequence	Best Mascot Ion Score		
			FLS2-GFP ctrl	FLS2-GFP flg22	Lti6B-GFP
MAPKKK7/6	AT3G13530.1/ AT3G07980.1	(R)GIPVLVGFLEADYAK(Y)	-	27.8	-
MAPKKK7	AT3G13530.1	(K)HITGIER(H)	-	28.5	-
MAPKKK7/6	AT3G13530.1/ AT3G07980.1	(R)SGGQVLVK(Q)	-	40.5	-
MAPKKK7/6	AT3G13530.1/ AT3G07980.1	(K)VADLLEFAR(A)	-	50.1	-
MAPKKK7	AT3G13530.1	(K)TLAVNGLTPLLISR(L)	-	78	-
MAPKKK7	AT3g13530.1	(R)HGGGEESHASTSN SQR(S)	22		20.3

16

1

2 **Table 1 FLS2-GFP co-immunoprecipitates with MKKK7.**

Protein name	Protein accession numbers	Peptide sequence	Best Mascot Ion Score		
			FLS2-GFP ctrl	FLS2-GFP flg22	Lti6B-GFP
MAPKKK7/6	AT3G13530.1/ AT3G07980.1	(R)GIPVLVGFLEADYAK(Y)	-	27.8	-
MAPKKK7	AT3G13530.1	(K)HITGIER(H)	-	28.5	-
MAPKKK7/6	AT3G13530.1/ AT3G07980.1	(R)SGGQVLVK(Q)	-	40.5	-
MAPKKK7/6	AT3G13530.1/ AT3G07980.1	(K)VADLLLEFAR(A)	-	50.1	-
MAPKKK7	AT3G13530.1	(K)TLAVNGLTPLLISR(L)	-	78	-
MAPKKK7	AT3g13530.1	(R)HGGGEEPSHASTSN SQR(S)	22		20.3

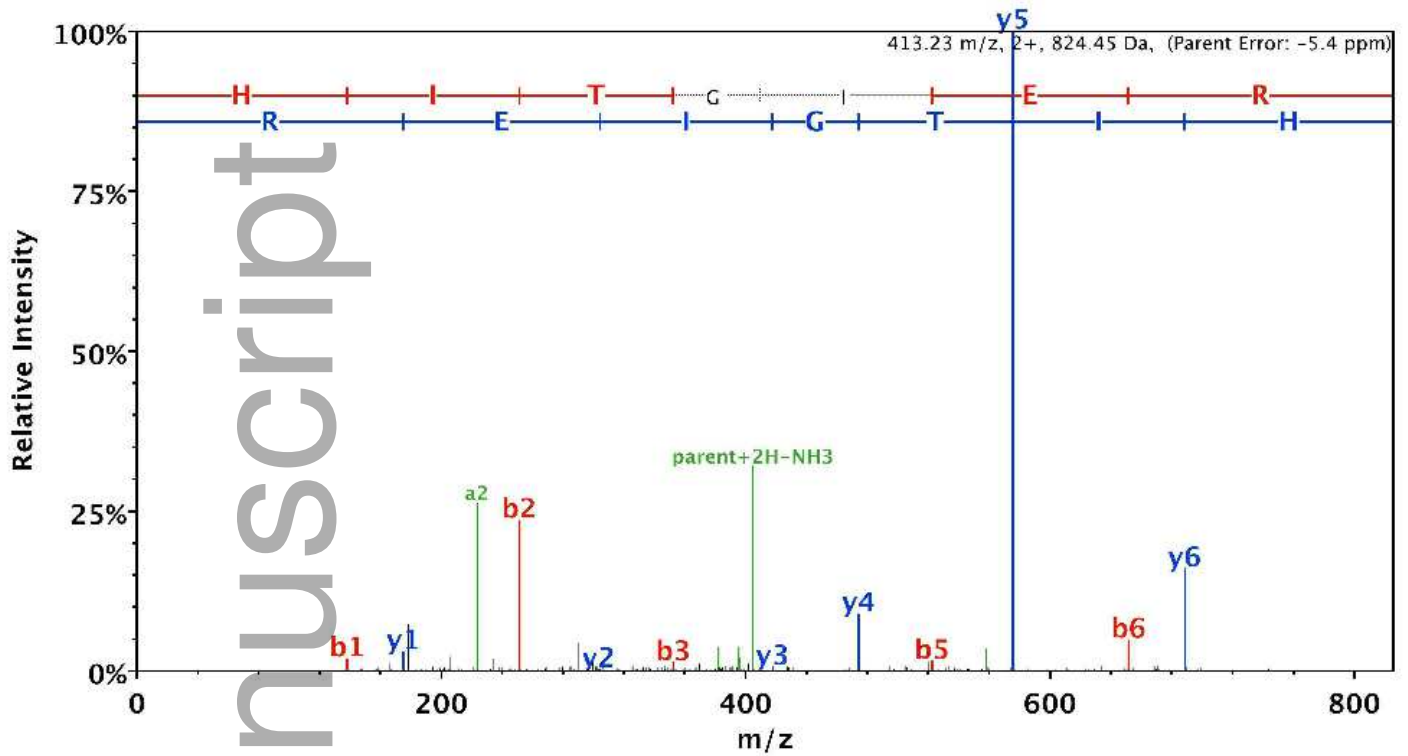
3

m/z 413.23, 2+

emb_201540806_1ev.pdf

A

HITGIER
b1 b2 b3 b5 b6



B

m/z 573.83, 2+

VADLLEFAR
b2 b3 b4 b5 b6 b7 b8 b9

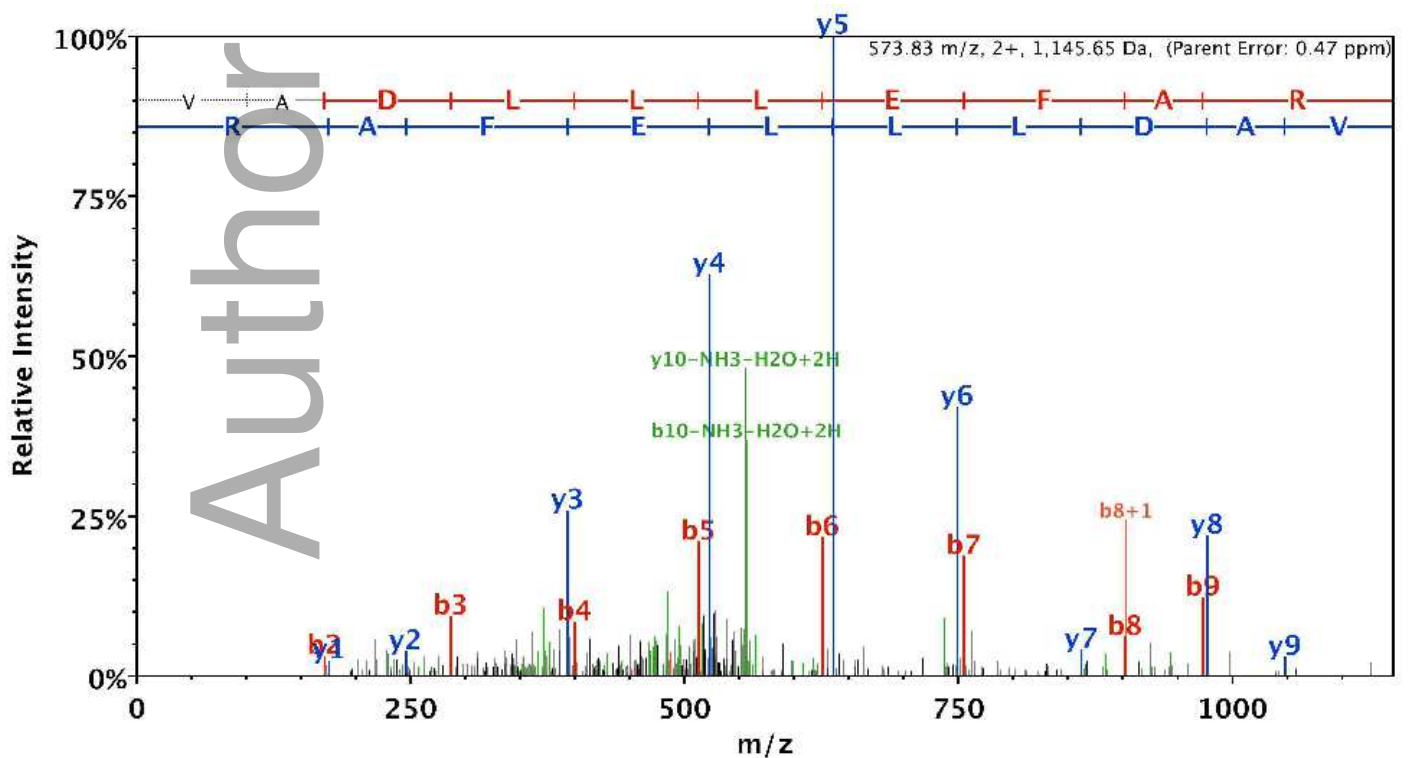


Figure EV1. Mithoe et al. This article is protected by copyright. All rights reserved

A



B

Pre-proof

MA	ROMTSSQF	HKSKTLDNKY	MLGDEIGKGA	YGRVYKGLDL	ENGDFVAIKQ
VS	LENIVOED	LNTIMOEDL	LKNLNHNKIV	KYLGSSSKTKT	HLHIILEYVE
NG	SLANI IKP	NKFGPFPEL	VAVYIAOVLE	GLVYLHEOGV	IHRDIKGANI
LT	TKEGLVKL	ADFGVATKLN	EADVNTHSVV	GTPYWMAPEV	IEMSGVCAAS
DI	WSVGCTVI	ELLTCVPPYY	DLOPMPALFR	IVODDNPPIP	DSLSPDITDF
LR	OCFKKDSR	ORPDAKTLLS	HPWIRNSRRA	LOSSLRHSGT	IKYMK EATAS
SE	KDDEGSQD	AAESLSGENV	GISKTDSSK	LPLVGVSSFR	SEKDQSTPSD
LG	EETDNSE	DDIMSDOVPT	LSIHEKSSDA	KGTPODVSDF	HGKSERGETP
EN	LVTETSEA	RKNTSAIKHV	GKELSIPVDO	TSHSFGRKGE	ERGIRKAVKT
PS	SVSGNELA	RFSDPPGDAS	LHDLFHPLDK	VSEGKPNEAS	TSMPTSNVNO
GD	SPVADGGK	NDLATKLRAT	IAQKQMEGET	GHSNDGGDLF	RLMMGVLKDD
VI	DIDGLVFD	EKVPAENLFP	LOAVEFSRLV	SSLRPDESED	AIVSSCOKLV
AM	FRORPEOK	VVFVTOHGFL	PLMDLLDIPK	SRVICAVLQL	INEI IKDNTD
FO	ENACLVLG	IPVVMFSAGP	ERDRSREIRK	EAAVFLOOLC	OSSPLTLOMF
IAC	RGI PVLV	GFLEADYAKY	REMVHLAIDG	MWOVFKLKRS	TPRNDFCR IA
AK	NGILLRLI	NTLYSLNEAT	R LASISGGLD	GOAPRVRSGQ	LDPNNPIFGQ
NET	SSLSPID	OPDVLKTRHG	GGEEPSHAST	SNSORSDVHO	PDALHPDGDK
PRV	SSVAPDA	STSGTEDVRO	OHRISLSANR	TSTDKLOKLA	EGASNGFPVT
OT	EOVRPLLS	LLDKEPPSRH	YSGQLDYVKH	ITGIERHESR	LPLLHGSNEK
KN	NGDLDFLM	AEFAEVSGRG	KENGSLDTTT	RYPSKTMTKK	VLAIEGVAST
SG	IASOTASG	VLSGSGVLNA	RPGSATSSGL	LAHMOVSTLSA	DVAREYLEKV
AD	LLLEFARA	DTTVKSYMCS	QSLLSRFLQM	FNRVEPPILL	KILECTNHLS
TD	PNCLLENLO	RADA IKHLIP	NLELKDGHV	YOIHHEVLSA	LFNLCKINKR
RO	EOAAENGI	IPHLMLFIMS	DSPLKOYALP	LLCDMAHASR	NSREOLRAHG
GL	DVYLSLLD	DEYWSVIALD	SIAVCLAQDN	DNRKVEQALL	KODAIQKLV
FE	OSCPERHF	VHILEPFLKI	ITKSYRINKT	LAVNGLTPLL	ISRDLHODAI
AR	LNLKLIK	AVYEHPRPK	QLIVENDLPQ	KLQNLIEERR	DGQRSGGQVL
VK	QMATSLLK	ALHINTIL			

This article is protected by copyright. All rights reserved

AtMKKK6 | NP_187455 SEKDAE-GSQEVVESVSAEKVEVTKTNS-----KSKLPVIGGASFRSEKDQSSPSDLGEE 354
 BnM3KE1 | XP_013686392 SEKDAE-GSEEVTELSSEKAGMSKSDS-----KSKL---GVASFRSEKDPSSSSDLGEE 351
 Csm3KE | XP_010465194 SEKDEE-GNQDVAESLSAENVMGSETDS-----KSKLPLVGVAEFRSEKDQTPPSDLGED 354
 AtMKKK7 | NP_187962 SEKDEE-GSQDAAESLSAENVMGSKSDS-----KSKLPLVGVSEFRSEKDQSTPSSDLGEE 354
 AlMKKK7 | XP_002884970 SEKDEE-GSQDAAESLSAENVMGMSKSDS-----KSKLPLLVGVSEFRSEKDQSTPSSDLGEE 350
 SlM3KE | NP_001234779 IREASNEEDKGAAGSSSDKAKESSTTL-----ASPEVLETSKSEEVDGASSIRIEG 352
 Nbm3KE | ADK36643 DTDASNEDDKGAAGSSSDKAKESCSVL-----ASPEVSEISKSEFDGSTSNHLEG 352
 Mdm3KE | XP_008340454 GAEISNGDNQGSAPSAEKVEVAASTIKADSGKELLSTEVPDMGRSDDNPASDVKSVEE 357
 Ptm3KE | XP_002307180 BAEILTGDNQRVTQINSVDRTKASVADFKAGSRKESLP-DSEVDVSKSDKNTSSDGDVVEE 358

AtMKKK6 | NP_187455 LETEASEGRRNTLATKLVGKE-YSIQSS---HSFSQKGE-DGLRKAVKTPSSVFGGNELTR 466
 BnM3KE1 | XP_013686392 SETESSKNGKNT-LEKQVGKE-SSIHVDQPSHVSQKGEDRRLRKAVRTPSSVGGNELTR 462
 Csm3KE | XP_010465194 LETEASEARKN---KQVGKE-CSIQVDQTSKSSGLKGEDRIRKAVKTPSSVGGNELTR 464
 AtMKKK7 | NP_187962 LVTETSEARKNTSAIKHVGE-LSIPVDQTSKSSFGKGEERGIRKAVKTPSSVSGNELAR 461
 AlMKKK7 | XP_002884970 LETETSEARKNTSAKQVGE-LSIPVDQTSKSSFGKGEERGIRKAVKTPSSVSGNELAR 457
 SlM3KE | NP_001234779 GELESSESRRNTVGRKVEDKGHVNAYSASSSSGQKNTDYSPRKAVKTSVVPQGNELSR 467
 Nbm3KE | ADK36643 GELESSESCKGNNVGRKKEEEKARGINAYSASSSSGQKNPDPHSPRKAMKISVVRGNELSR 467
 Mdm3KE | XP_008340454 GEVRSPELTKNVSGKQGGK----GVGYRAFQFGRNODGSGFKAAKMPVLLGGNELSK 471
 Ptm3KE | XP_002307180 DDLESPDARGKNIERNNGKTSS-ARVENSFGFATRNDGLRKAOKVKTSMSTSGGNELSK 476

AtMKKK6 | NP_187455 FSDPPGDASLHDLFHPDKVPEGKTNEASTSTPTANVNQGDSPVADGGKNDLATKLRARI 526
 BnM3KE1 | XP_013686392 FSDPPGDASLHDLFQPLDKVPEGKNEASTSAPTNSVIQGDSPVADGGKNDLATKLRATI 522
 Csm3KE | XP_010465194 FSDPPGDASLHDLFHPDKVPEGKNEASTSMPTSNINQGDSPVADGGKNDLATKLRATI 524
 AtMKKK7 | NP_187962 FSDPPGDASLHDLFHPDKVSEGKNEASTSMPTSNVNQGDSPVADGGKNDLATKLRATI 521
 AlMKKK7 | XP_002884970 FSDPPGDASLHDLFHPDKVSEGKNEASTSMPTSNVNQGDSPVADGGKNDLATKLRATI 517
 SlM3KE | NP_001234779 FSDPPGDASLDDLHHPLEKNLENRAAEVLSASSSQIAQNNAI-AETGKNDLATKLRATI 526
 Nbm3KE | ADK36643 FSDPPGDASLDDLHHPLEKNLENRAAEVLSASSSQIAQNSAV-SETGKNDLATKLRATI 526
 Mdm3KE | XP_008340454 FSDTPGDASLDDLHHPDKHPEDRTEASTSASMSQSNQGNTPGNDAGKSDLATKLRATI 531
 Ptm3KE | XP_002307180 FSDTPRDASLDDLHHPDKNPEDRAAEASTSTASAHMNOGNAIMADAGKNDLAAILRATI 536

AtMKKK6 | NP_187455 NTLYSLSEATRLASISG-DALILDQGTFRARSGQLDPNPNPIFSQRET-SPSVIDHPDGLK 823
 BnM3KE1 | XP_013686392 NTLYSLNEATRLASISG-GPLSVDGLAPRLRSGQLDPNPNPIFSHHES-SLGVIDHPDALK 819
 Csm3KE | XP_010465194 NTLYSLNEATRLASISG-GALIVDQAPRVRSGQLDPNPNPIFTQHET-SLSMIDQPDVVK 821
 AtMKKK7 | NP_187962 NTLYSLNEATRLASISG-G---LDGQAPRVRSGQLDPNPNPIFGQNETSLSMIDQPDVVK 816
 AlMKKK7 | XP_002884970 NTLYSLNEATRLASISG-GA-IVDQAPRVRSGQLDPNPNPIFGQNET-SLSMIDQPDVVK 813
 SlM3KE | NP_001234779 NTLYSLNEAARLASASGGGGFPPDGLAPRPRSGPLDHGNSSFQTEV-PPYGTQPDMLK 821
 Nbm3KE | ADK36643 NTLYSLNEAARLASASGGGGFPPDGLAPRPRSGPLDPGNSSFMQTEM-PPYGTQPDMLK 821
 Mdm3KE | XP_008340454 NTLYSLNEATRLASISVGGGFPLEGSAQRPRSGSLDSGHPIFAQSDV-LLSTTDQHDLK 828
 Ptm3KE | XP_002307180 NTLYSLNEATRLASISVGTGFPLDGLSQRPDSGPLDSNHPIFIQSET-ALSASDQPDVFK 832

AtMKKK6 | NP_187455 TRNG-----GGEESHASTSNSQSSDVHQPDA--LHPDGRPRLLSSVVADA----- 867
 BnM3KE1 | XP_013686392 TKHV-----GGEESHASTSNSQSSDIHQ-----DGDRPRLSSAAADGS----- 859
 Csm3KE | XP_010465194 TRHG-----GGEESHASTSNSQSSDVHQPDA--LHPDGRPRLLSVPDASTS--- 868
 AtMKKK7 | NP_187962 TRHG-----GGEESHASTSNSQSSDVHQPDA--LHPDGDKPRVSSVAPDASTS--- 863
 AlMKKK7 | XP_002884970 TRHG-----VGEESHASTSNSQSSDVHQPDA--LHPDGRPRVSSVAPDASTS--- 860
 SlM3KE | NP_001234779 IKNGD--RVLPSGMQEPSSRNSASHS-----PDSPPFRQDGERPRSSNATMEASGLSRL 872
 Nbm3KE | ADK36643 IKNGE--RVLPAQMQLSRTSASHS-----PDSPYFRQDGERPRSSNATVEVSGPSKL 872
 Mdm3KE | XP_008340454 VRHGLIDFHLSTGTAEPARASTSNSQSSDANQSDPRYLHLLTDRAQSNVVEAIVPSKL 888
 Ptm3KE | XP_002307180 VRHGMIDHSLPFQTTLEPRASSTSHSQRDLAIQPDARFFGTDTDGSQASNETIEAIAASKL 892

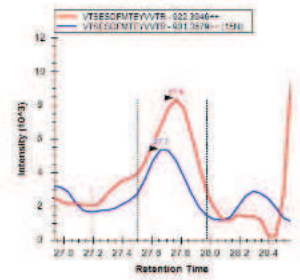
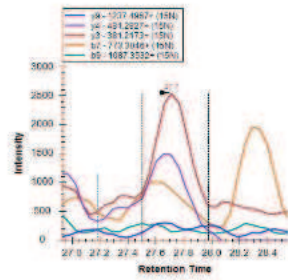
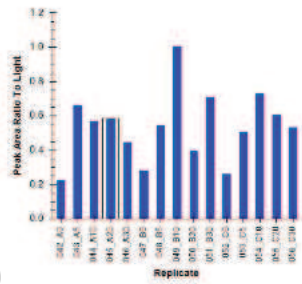
Author Manuscript
 Accepted Article

A

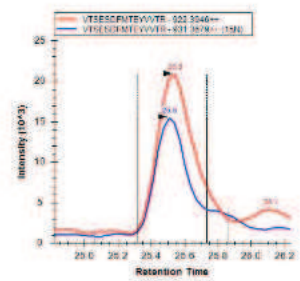
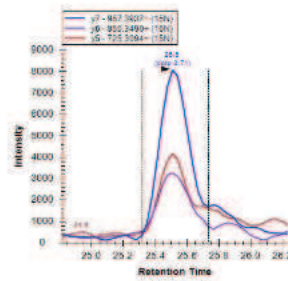
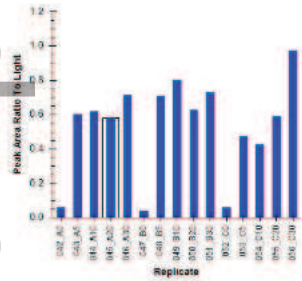
VTSESDFMpTEYVVTR

embr_201540806_f4ev.pdf
 Integrated peak areas ¹⁵N Transitions measured in sample (B5 example)

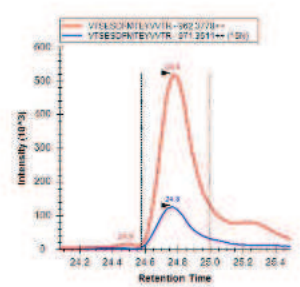
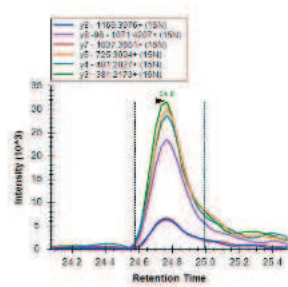
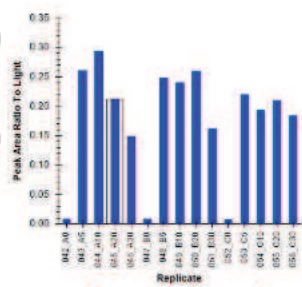
Total integrated peak area for light and heavy peptide in sample (B5 example)



VTSESDFMTEpYVVTR



VTSESDFMpTEpYVVTR



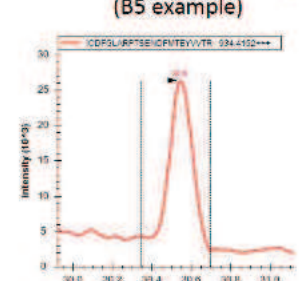
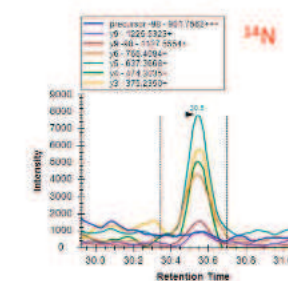
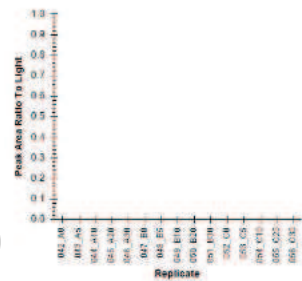
A B C

B

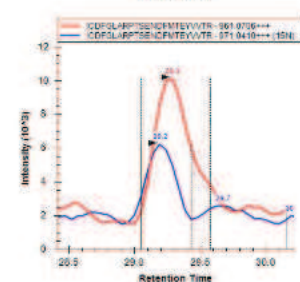
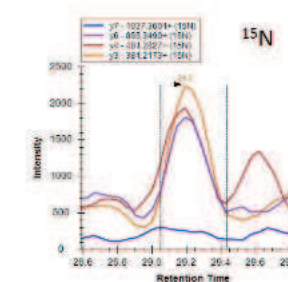
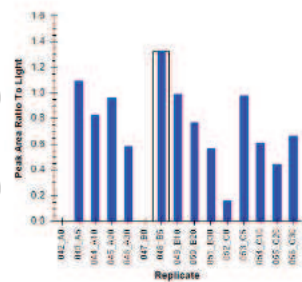
ICFGARPTSEDFMpTEYVVTR

Integrated peak areas ¹⁵N/¹⁴N Transitions measured in sample (B5 example)

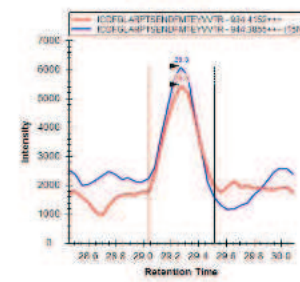
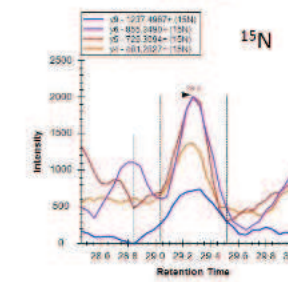
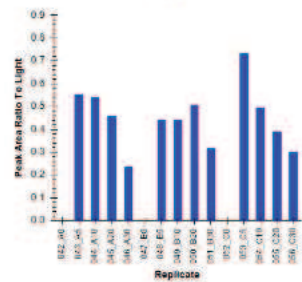
Total integrated peak area for light and heavy peptide in sample (B5 example)



ICFGARPTSEDFMTEpYVVTR



ICFGARPTSEDFMTEpYVVTR



A B C

This article is protected by copyright. All rights reserved

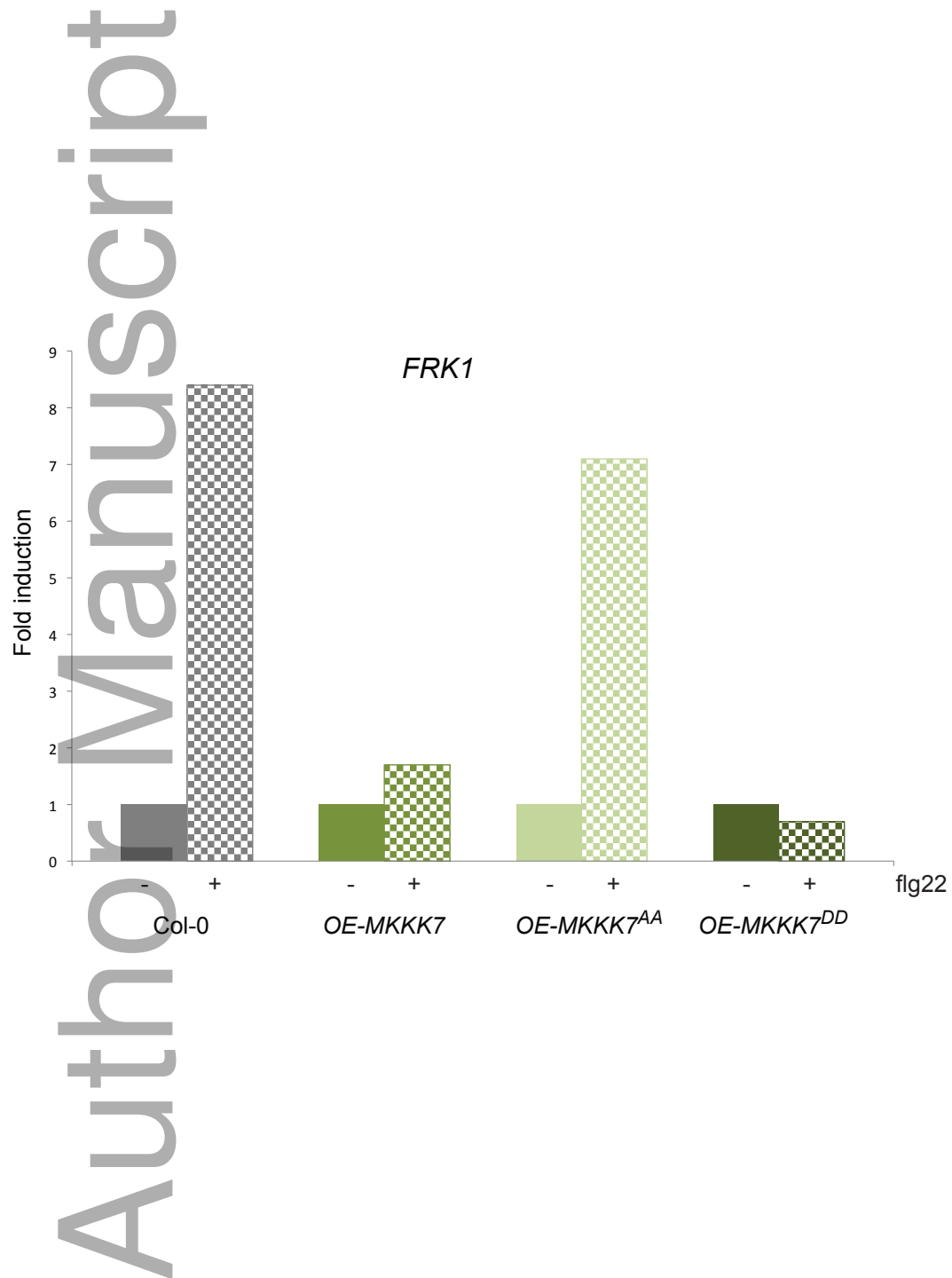
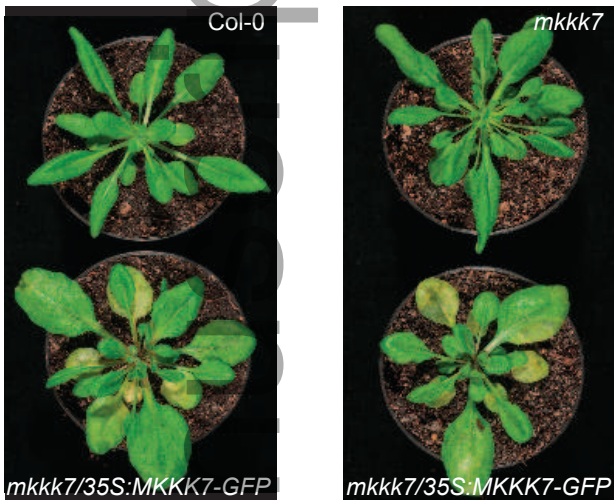
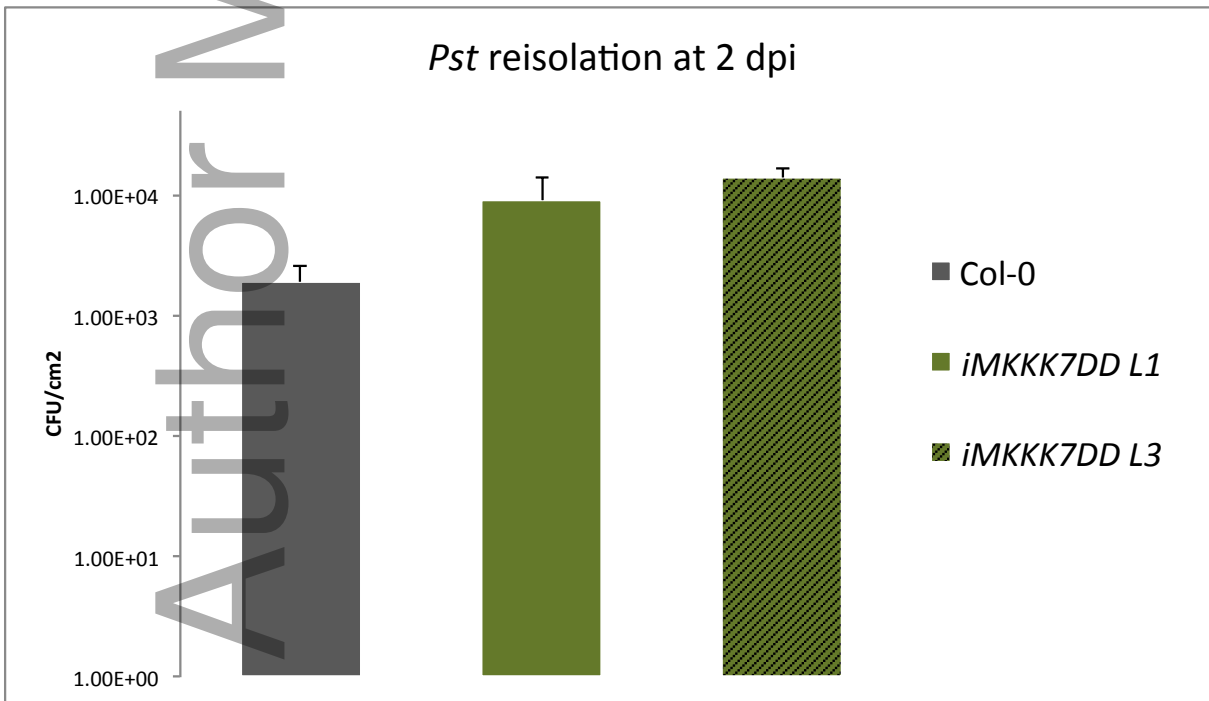


Figure EV5 ; Mithoe et al.,

A



B



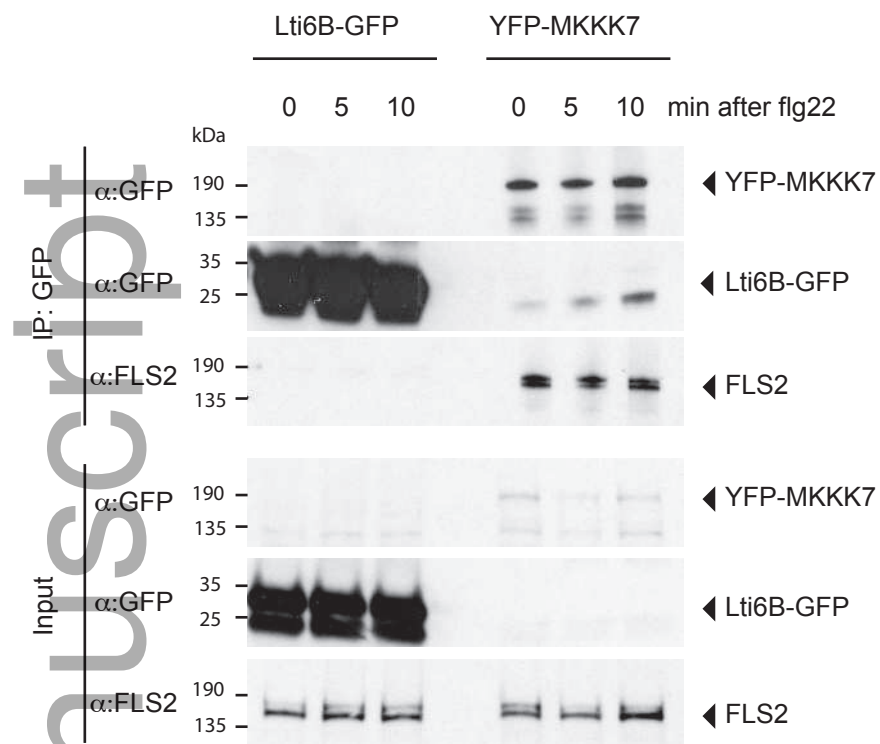


Figure 1, Mithoe et al.,

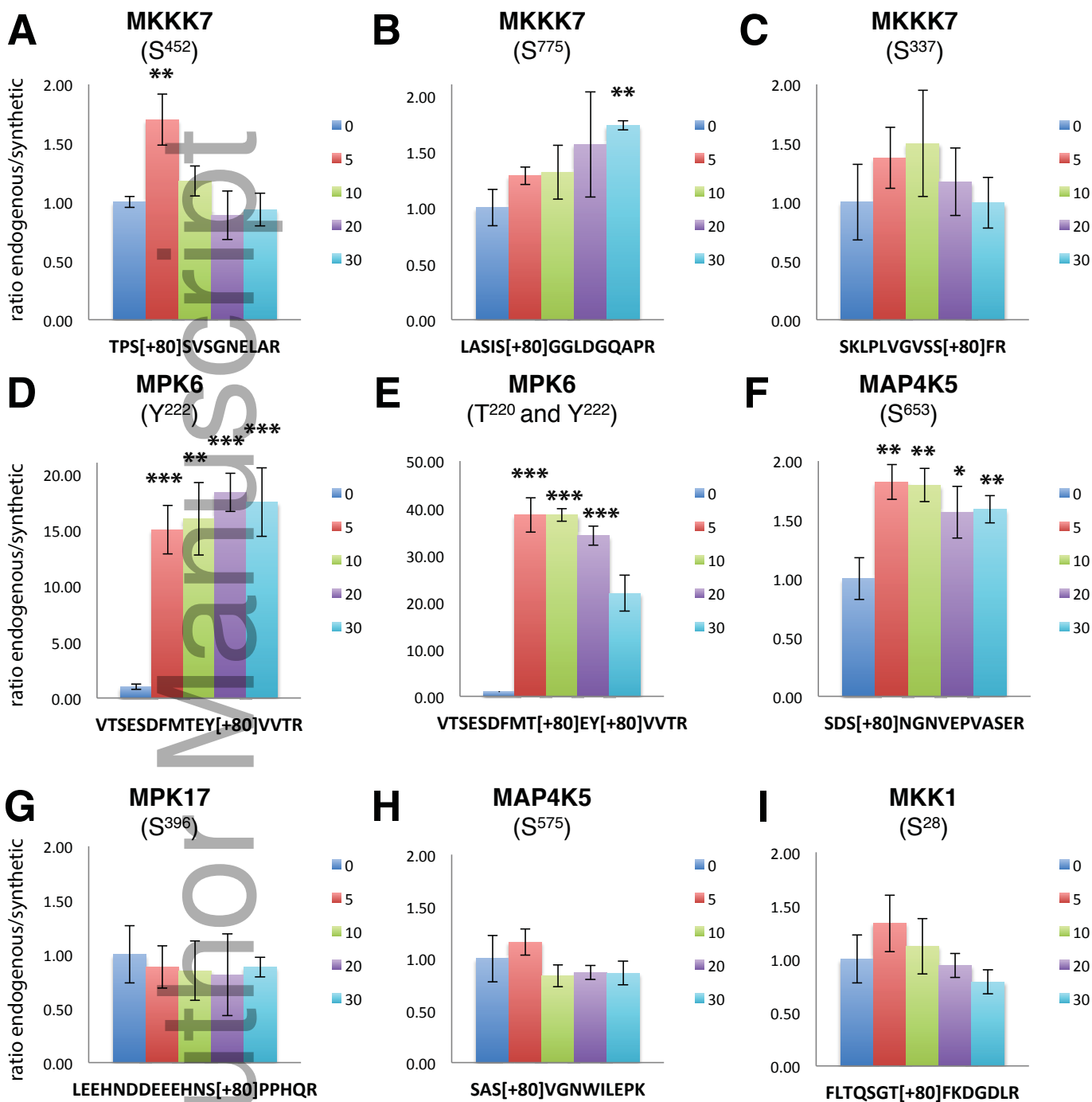
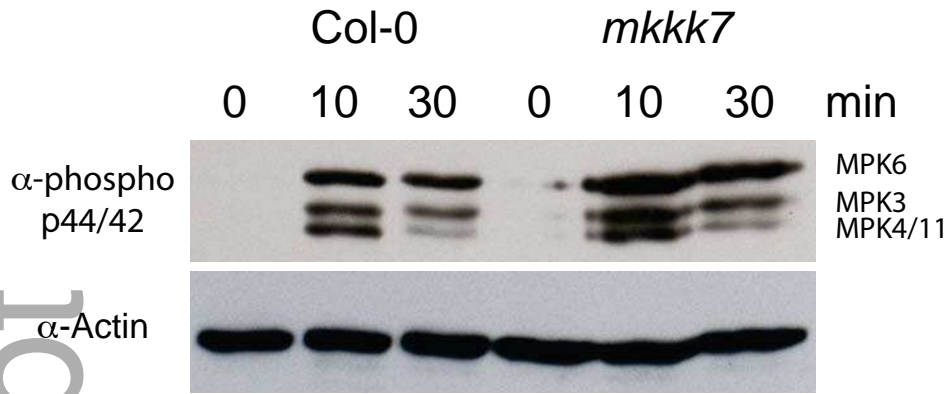


Figure2 , Mithoe et al.,

A



B

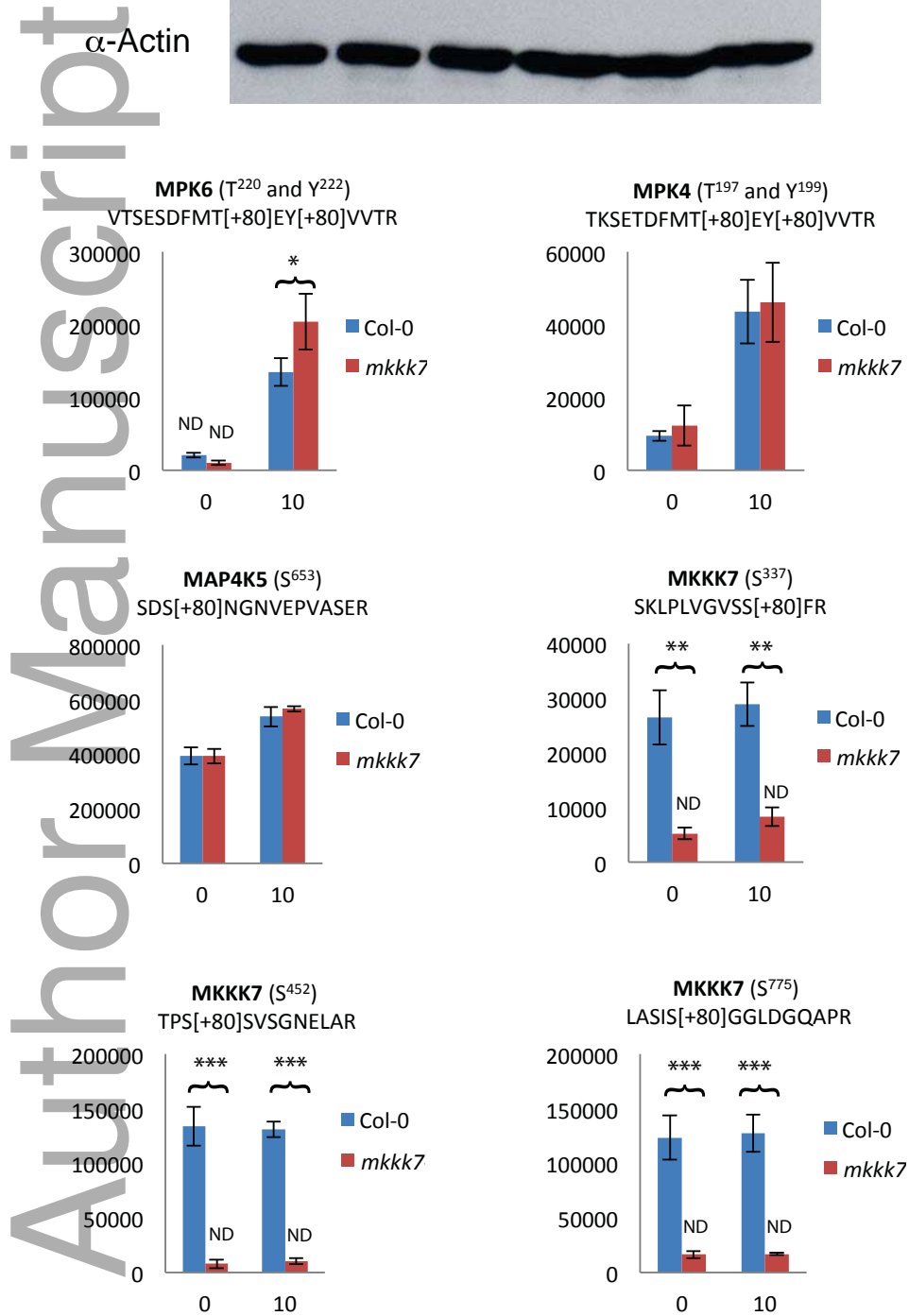


Figure 3, Mithoe et al.,

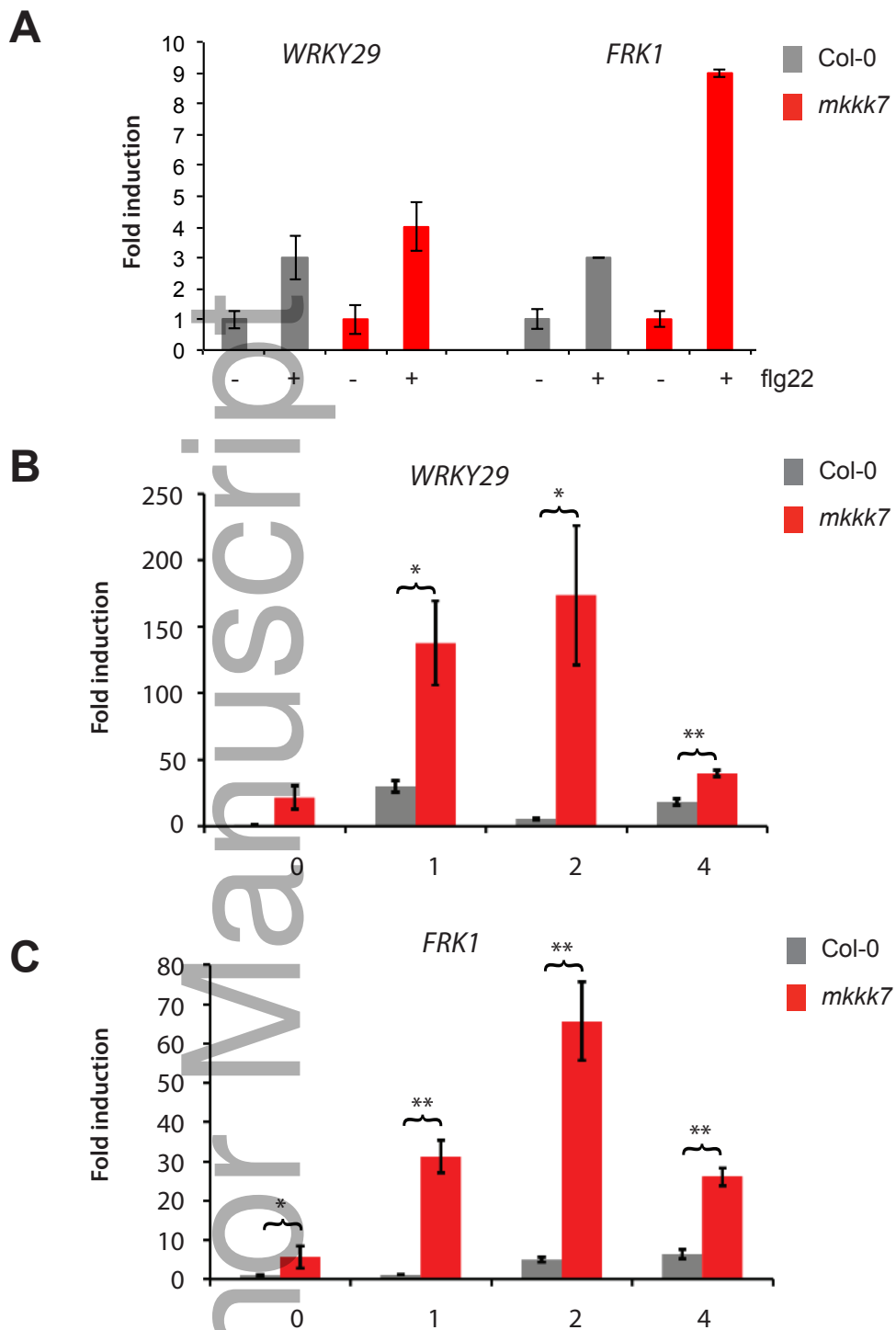


Figure 4, Mithoe et al.,

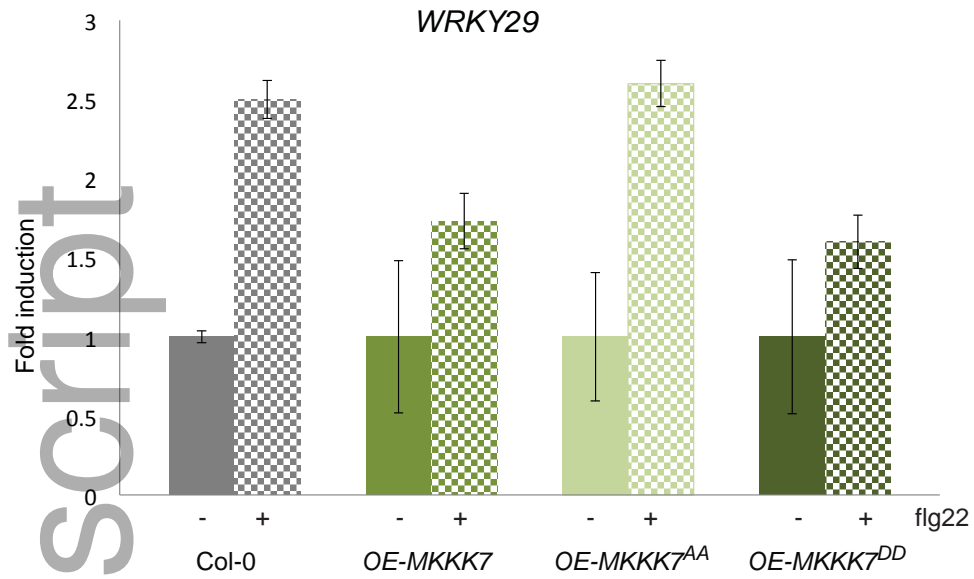
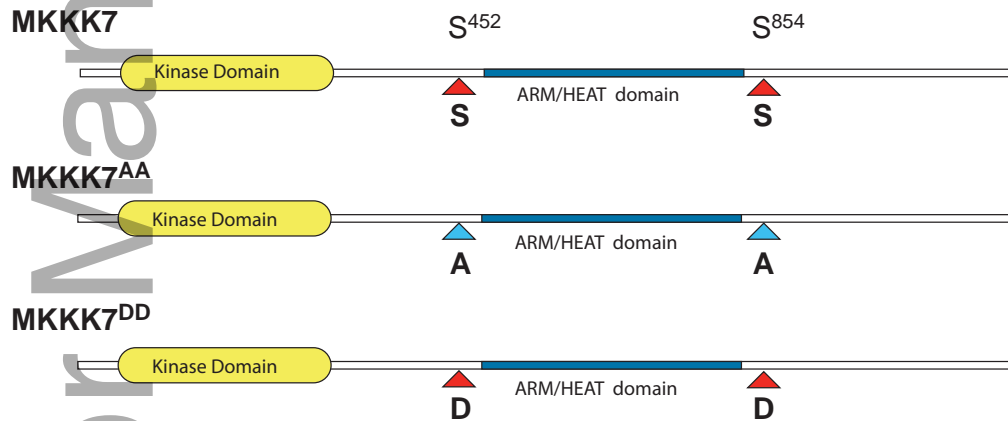
A**B**

Figure 5, Mithoe et al.,

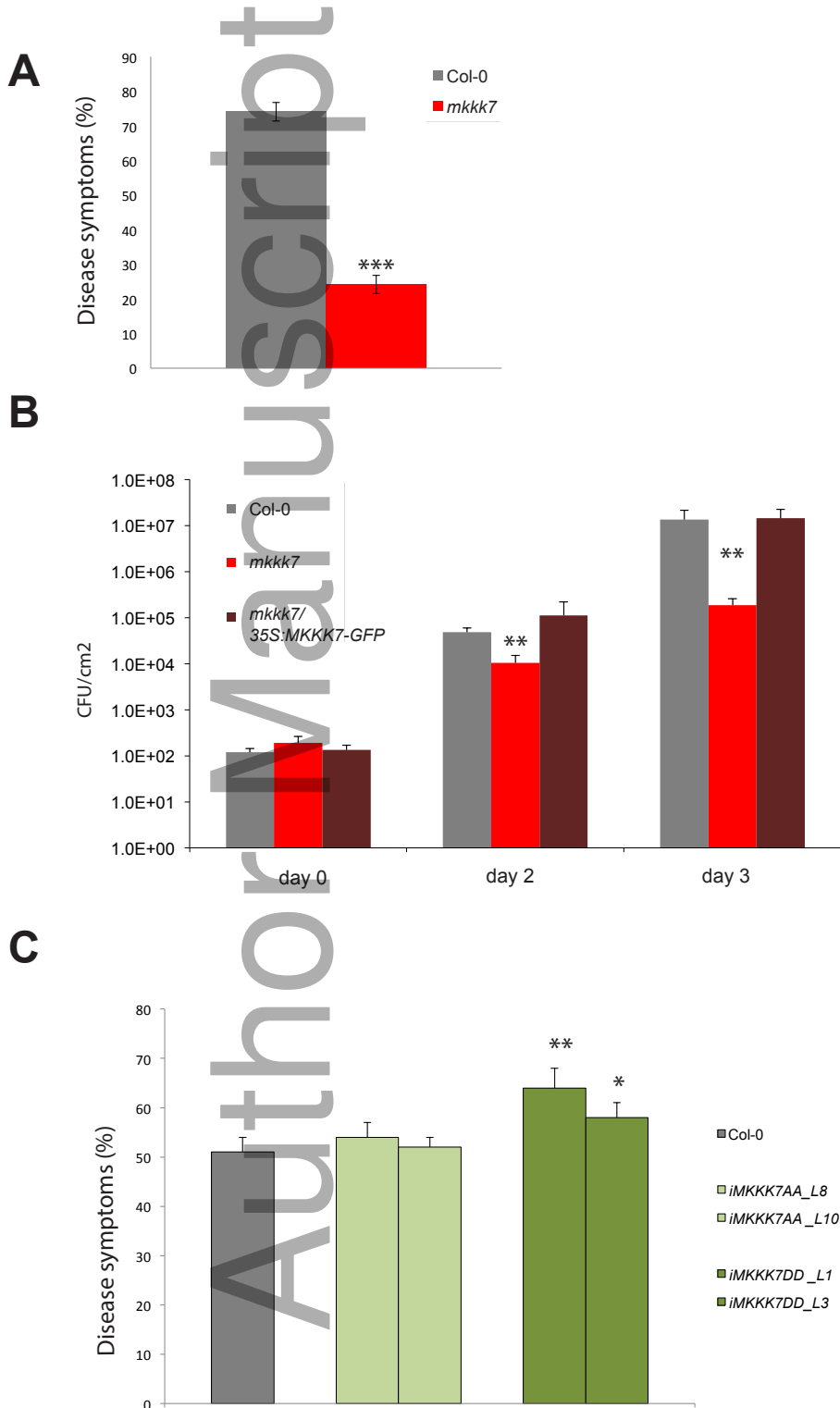
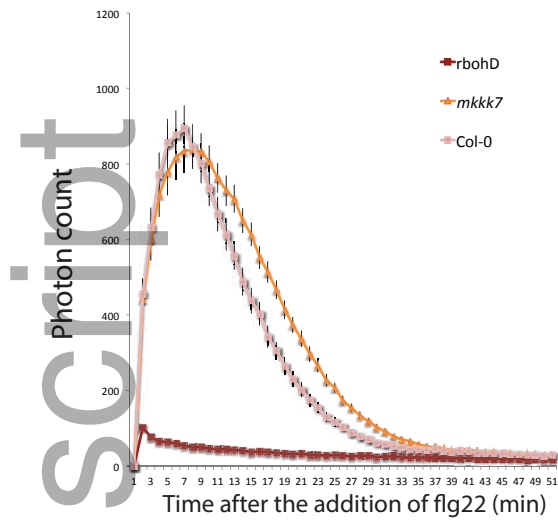
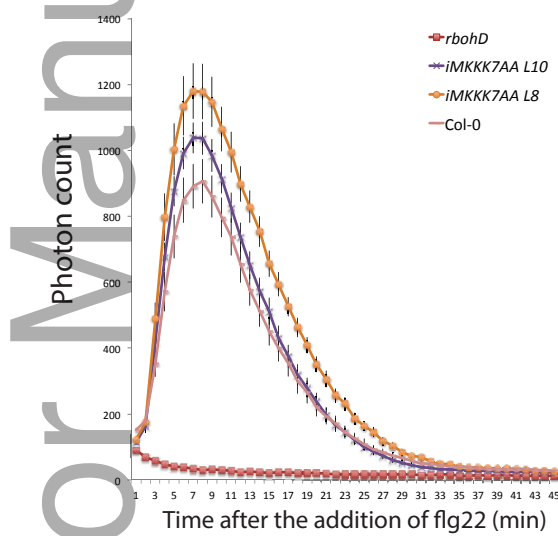
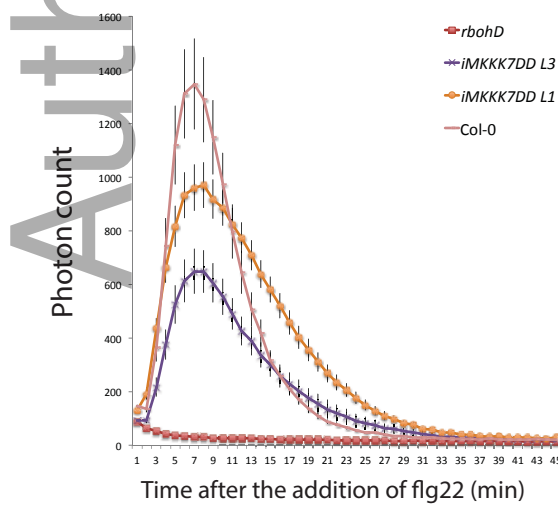


Figure 6, Mithoe et al.,
This article is protected by copyright. All rights reserved

A**B****C**

This article is protected by copyright. All rights reserved